J. Fluid Mech. (2000), *vol.* 404, *pp.* 211–250. Printed in the United Kingdom

Hydrothermal wave instability of thermocapillary-driven convection in a transverse magnetic field

By JĀNIS PRIEDE† AND GUNTER GERBETH
Forschungszentrum Rossendorf, P. O. Box 510119, 01314 Dresden, Germany

(Received 14 October 1998 and in revised form 27 September 1999)

We study the linear stability of thermocapillary-driven convection in a planar unbounded layer of an electrically conducting low-Prandtl-number liquid heated from the side and subjected to a transverse magnetic field. The thresholds of convective instability for both longitudinal and oblique disturbances are calculated numerically and also asymptotically by considering the Hartmann and Prandtl numbers as large and small parameters, respectively. The magnetic field has a stabilizing effect on the flow with the critical temperature gradient for the transition from steady to oscillatory convection increasing as square of the field strength, as also does the critical frequency, while the critical wavelength reduces inversely with field strength. These asymptotics develop in a strong enough magnetic field when the instability is entirely due to the jet of the base flow confined in the Hartmann layer at the free surface. In contrast to the base flow, the critical disturbances, having a long wavelength at small Prandtl numbers, extend from the free surface into the bulk of the liquid layer over a distance exceeding the thickness of the Hartmann layer by a factor $O(Pr^{-1/2})$. For $Ha \lesssim Pr^{-1/2}$ the instability is influenced by the actual depth of the layer. For such moderate magnetic fields the instability threshold is sensitive to the thermal properties of the bottom of the layer and the dependences of the critical parameters on the field strength are more complicated. In the latter case, various instability modes are possible depending on the thermal boundary conditions and the relative magnitudes of Prandtl and Hartmann numbers.

1. Introduction

Thermocapillary or Marangoni convection is a fluid flow driven by thermally induced variation of the surface tension. For common liquids, whose surface tension decreases with temperature, the surface is driven from hot to cold regions. Due to viscosity the surface motion spreads to the underlying liquid but incompressibility gives rise to a pressure gradient driving a return flow in the bulk of the liquid. Such flows can occur in systems with liquid–gas or liquid–liquid interfaces subject to a temperature gradient. There are several different ways in which the thermocapillary convection can take place. In the classical case, when the temperature gradient is strictly normal to the interface, the latter is at a constant temperature and, thus, in a static mechanical equilibrium, which becomes unstable as the temperature gradient exceeds some critical value (Davis 1987). The instability results in a steady cellular

† Present address: Institute of Physics, University of Latvia, Salaspils, Latvia; email priede@sal.lv.

convection (Pearson 1958) or in travelling surface waves (Takashima 1981) when the liquid is cooled or heated from the surface, respectively.

This paper is concerned with another arrangement where the temperature gradient is applied along the liquid surface. In this case convection starts immediately regardless of how small the temperature gradient is. Here the thermocapillarity plays a double role: besides driving the basic flow it can also be a cause of a dynamic instability called hydrothermal waves which arise as the longitudinal temperature gradient exceeds a certain threshold depending on the liquid properties and the geometry (Smith & Davis 1983*a*). Hydrothermal waves are coupled flow and temperature disturbances sustained by velocity and temperature gradients of the basic flow. Coupling of the flow and temperature fields through the surface tension is essential for this instability and this coupling makes it different from the usual hydrodynamic instability.

Thermocapillary-driven flows play an important role in several semiconductor crystal growth processes from the melt like Czochralski and the float-zone methods where a free surface of the melt is present (Schwabe 1988). The melt flow can significantly affect the homogeneity and purity of the crystals grown. Most crucial for the crystal growth is the steadiness of the flow. An oscillating melt motion leaves marks in the grown crystal in the form of dopant layers called striations which seriously deteriorate the quality of the produced crystals.

Because molten semiconductors possess the electrical conductivity of liquid metals, magnetic fields can be used to control the melt flow (Series & Hurle 1991). For several years this has been a motivation for a series of studies on the effect of magnetic fields on thermocapillary instabilities. So far, most attention has been paid to the onset of a steady Bénard–Marangoni convection in a planar unbounded liquid layer heated from below and subject to a transverse magnetic field. This problem is now well understood due to theoretical studies by Nield (1966), Sarma (1979), Maekawa & Tanasawa (1989) and Wilson (1993*a*): an increase of magnetic field results in a monotonic rise of the critical temperature gradient. In a strong magnetic field the critical temperature gradient and the critical wavenumber increase as the square and square root of the field strength, respectively (Wilson 1993*a*). However, the magnetic field cannot stabilize long-wave surface deformations which thus remain the most dangerous perturbations (Wilson 1993*a*). Oscillatory Marangoni convection caused by heating from the top in a magnetic field has been considered by Nitschke, Thess & Gerbeth (1991) and Wilson (1993*b*). This instability can effectively be suppressed by a relatively weak magnetic field. Hydrothermal wave instability in a magnetic field parallel to the liquid layer was the subject of our previous study (Priede & Gerbeth 1997*a*). Such a magnetic field has a stabilizing effect on all disturbances except those aligned with the field which are not influenced at all. In the case of a parallel magnetic field the most effective stabilization is provided by the field spanwise to the basic flow. However, more effective stabilization is provided by a magnetic field transverse to the liquid layer which in contrast to the coplanar one effectively retards the basic flow. Until now the influence of a transverse magnetic field has been considered only on the longitudinal hydrothermal waves (Priede, Thess & Gerbeth 1994) which, however, are not the most dangerous perturbations.

In this paper we present a detailed study of the effect of a transverse magnetic field on both longitudinal and oblique hydrothermal wave instabilities of a thermocapillary-driven flow in a planar unbounded layer of an electrically conducting liquid heated from the side. For longitudinal waves the dispersion relation is found in an analytic form which is solved numerically for neutrally stable modes. For non-longitudinal disturbances the linear stability problem is solved completely numerically. However,

numerical results alone often do not provide the most valuable information contained in the solution of such an idealized problem such as considered here. Particular numerical values for real applications and this simple model may be quite different, though the physical mechanisms and the dependence between the parameters characterizing them may still be the same. This information is contained in scaling relations which are not always obvious from the numerical solution. To obtain the relevant scalings we resort to an order of magnitude analysis. We use the order of magnitude estimates or implications from the numerical results, when the first are not simply obtainable, to solve the problem asymptotically. The asymptotic solution is complicated by the presence of two dimensionless parameters in the problem: the Prandtl number, the ratio of the heat conductivity and the kinematic viscosity, which is typically small $O(10^{-2})$ for semiconductor melts and liquid metals, and the Hartmann number Ha characterizing the strength of the magnetic field, which may be large $O(10^2)$. There are a number of asymptotic solutions possible depending on the relative magnitude of both parameters taken to certain powers. For instance, if $1 \ll Ha \ll Pr^{-1/2}$ the asymptotic solutions differ depending on the thermal boundary conditions at the bottom of the layer. For $Ha \gg Pr^{-1/2}$, there is another asymptotic solution independent of the thermal boundary conditions.

For the most dangerous oblique waves, an asymptotic solution is obtained by combining analytical and numerical approaches. In the case of strong magnetic field, a direct numerical solution is often complicated by the presence of very different length scales in the problem. There is a thin Hartmann layer developing at the free surface where the basic flow is confined and a complicated interaction between the disturbances occurs. For small Prandtl numbers, the critical wavelength is typically much longer than the characteristic thickness of the Hartmann layer. Thus disturbances extend far outside the Hartmann layer. It is not simple for numerics to resolve two such very different length scales. On the other hand, because outside the Hartmann layer the basic flow is almost suppressed, the disturbance equations there are relatively simple and can be solved analytically for oblique waves also. This analytic solution in the outer region can effectively be combined with the numerical solution in the boundary layer. As a result, we obtain a series of simple expressions for the instability parameters which besides containing scaling information also provide a satisfactory approximation to the full numerical solution.

The layout of the paper is as follows. Section 2 presents the problem formulation. Longitudinal waves are analysed in § 3 with Hartmann-layer and finite-depth modes for insulating and conducting bottom walls considered in §§ 3.1, 3.2 and 3.3, respectively. For an insulating bottom there are two finite-depth instability modes found with critical frequencies lower and higher, respectively, than the inverse thermal relaxation time over the depth of the layer. Details of the asymptotic solutions for these modes are presented in the Appendix, §§ A.1.1 and A.1.2. An asymptotic solution for the finite-depth longitudinal waves in the case of a perfectly conducting bottom is obtained in the Appendix, § A.2. Oblique waves are considered in § 4 with §§ 4.1, 4.2, and 4.3 devoted to the Hartmann-layer and finite-depth modes for insulating, and conducting bottoms, respectively. Section 5 contains summary of the work and some concluding remarks.

2. Formulation of the problem

Consider an unbounded horizontal layer of viscous electrically conducting liquid of density ρ, kinematic viscosity ν, thermal conductivity κ and electric conductivity σ.

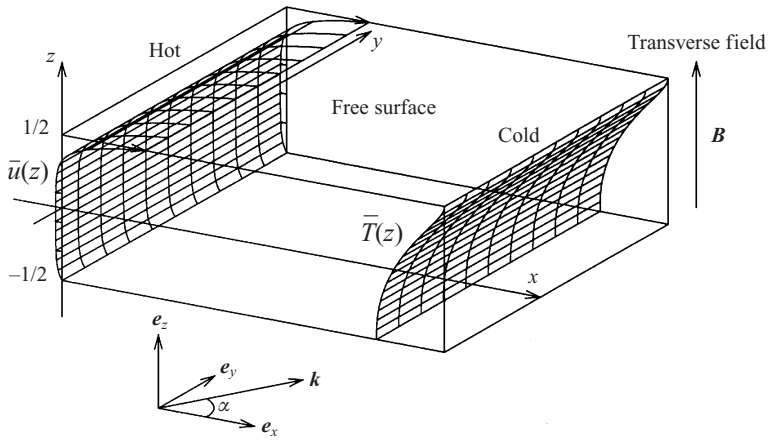

FIGURE 1. Sketch of the model with the basic velocity and temperature profiles.

The layer having depth d at rest is bounded from below by a plane perfectly electrically insulating plate, and above by a free surface. The bottom of the layer is assumed to be either perfectly thermally insulating or conducting while the free surface is considered as an adiabatic boundary. A constant temperature gradient β is imposed along the layer, and a steady shear flow is set up by temperature-dependent surface tension which is assumed to vary according to the linear law $\tau = \tau_0 - \gamma(T - T_0)$, where $\gamma = -\mathrm{d}\tau/\mathrm{d}T > 0$ is the negative rate of change of surface tension with temperature; τ_0 and T_0 are reference values for surface tension and temperature, respectively. The flow is subjected to a uniform magnetic field of induction $\boldsymbol{B} = \boldsymbol{e}_z B$ transverse to the liquid layer. As shown in figure 1, the origin of the Cartesian coordinate system is set at mid-height of the layer with the x-axis directed oppositely to the imposed temperature gradient and the z-axis normal to the plane of the layer. The depth d is assumed to be small enough so that buoyancy can be neglected in comparison to thermocapillary effects. The surface tension is assumed to be high enough so that the free surface may be considered as a planar and non-deformable boundary. The distortion of the external magnetic field by the fluid flow is neglected in accordance with the inductionless or low magnetic Reynolds number approximation commonly employed in laboratory magnetohydrodynamics (Moreau 1990).

Transforming the governing equations and boundary conditions to a dimensionless form the depth d is chosen as length scale, and the time t, velocity field v, pressure field p, temperature difference $T - T_0$, and the induced electrostatic potential ϕ are referred to scales d^2/ν, ν/d, $\rho\nu^2/d^2$, βd, and $B\nu$, respectively. The phenomena under consideration are governed by the Navier–Stokes equation with an electromagnetic force term added, the incompressibility constraint, the energy equation and the continuity equation for electric current

$$\partial_t \boldsymbol{v} + (\boldsymbol{v}\cdot\nabla)\boldsymbol{v} = -\nabla p + \nabla^2\boldsymbol{v} + Ha^2(-\nabla\phi + \boldsymbol{v}\times\boldsymbol{e}_z)\times\boldsymbol{e}_z, \tag{2.1}$$

$$\nabla\cdot\boldsymbol{v} = 0, \tag{2.2}$$

$$\partial_t T + \boldsymbol{v}\cdot\nabla T = Pr^{-1}\nabla^2 T, \tag{2.3}$$

$$\nabla^2\phi = \boldsymbol{e}_z\cdot\nabla\times\boldsymbol{v}, \tag{2.4}$$

where $Ha = Bd(\sigma/\rho\nu)^{1/2}$ is the Hartmann number, and $Pr = \nu/\kappa$ is the Prandtl number. The mechanical boundary conditions on the free surface $z = \frac{1}{2}$ are $\boldsymbol{e}_z\cdot\boldsymbol{v} = 0$

and

$$\boldsymbol{e}_z \times (\partial_z \boldsymbol{v} + Re \nabla T) = \boldsymbol{0}, \tag{2.5}$$

where $Re = \gamma \beta d^2/\rho \nu^2$ is the Reynolds number. In fact, condition (2.5) represents the sole driving force for the convective flow considered here: the balance between thermocapillary and viscous stresses at the free surface. For consistency with previous papers on this subject we use also the Marangoni number $Ma = RePr$ in addition to the Reynolds number. So the Marangoni number is not an independent parameter and it is used only for the convenience of representation of the results.

The free surface is assumed to be an adiabatic boundary

$$\partial_z T = 0 \quad \text{on } z = \tfrac{1}{2}.$$

On the rigid lower boundary, there are conditions of no slip, impermeability and zero heat flux in the case of thermally insulating bottom

$$\boldsymbol{v} = \boldsymbol{0}; \quad \partial_z T = 0 \quad \text{on } z = -\tfrac{1}{2},$$

or a fixed temperature for perfectly thermally conducting bottom

$$T(-1/2) = T_\infty(x) = -x.$$

Subsequently these two boundary conditions will be referred to as insulating and conducting ones. At both boundaries, assumed to be electrically insulated, the normal component of the induced electric current must vanish

$$j_n = -\partial_z \phi = 0 \quad \text{on } z = \pm\tfrac{1}{2}. \tag{2.6}$$

The system (2.1)–(2.6) has a steady parallel flow solution $\bar{\boldsymbol{v}} = (\bar{u}, 0, 0)$ maintaining zero mass flux through any vertical cross-section. Neglecting exponentially small terms for strong magnetic field ($Ha \gg 1$) this solution takes the simple form

$$\bar{u}(z) = Re \left(\frac{\exp(-(\frac{1}{2} - z)Ha)}{Ha} + \frac{\exp(-(\frac{1}{2} + z)Ha) - 1}{Ha^2} \right), \tag{2.7}$$

$$\bar{T}(x, z) = -x - PrRe \left(\frac{\exp(-(\frac{1}{2} - z)Ha) - \frac{1}{2}z(z+1)Ha}{Ha^3} + \frac{\exp(-(\frac{1}{2} + z)Ha) + zHa}{Ha^4} \right), \tag{2.8}$$

$$\bar{p}(x) = Re\, x, \qquad \bar{\phi}(z) = 0. \tag{2.9}$$

At large Hartmann numbers, the basic flow forms a jet at the free surface. Both the characteristic thickness and the velocity of the jet decrease with the magnetic field as $\sim Ha^{-1}$. The constant pressure gradient drives a return flow in the core region which is separated by the jet from the free surface and by the Hartmann layer from the bottom. The return flow has a uniform velocity $\sim Ha^{-2}$.

We analyse the linear stability of the basic state (2.7)–(2.9) with respect to infinitesimal disturbances in the form of a plane travelling wave

$$(\boldsymbol{v}, p, T, \phi) = (\bar{\boldsymbol{v}}, \bar{p}, \bar{T}, \bar{\phi}) + \{\hat{\boldsymbol{v}}(z), \hat{p}(z), \hat{T}(z), \hat{\phi}(z)\} \exp(\mathrm{i}\boldsymbol{k} \cdot \boldsymbol{r} + \lambda t),$$

where $\boldsymbol{k} = (k_x, k_y)$ and $\boldsymbol{r}$ are wave and radius vectors, respectively; λ is a complex growth rate. Upon substituting the solution sought in such a form into the governing equations (2.1)–(2.4) and applying the *curl* operator twice to (2.1) in order to eliminate

both the pressure and the scalar potential, the equations for the remaining disturbance amplitudes may be written as

$$\lambda \mathbf{D}^2 \hat{w} = \left[\mathbf{D}^4 - Ha^2(\boldsymbol{e}_z \cdot \mathbf{D})^2\right] \hat{w} - \mathrm{i}k_x \left[\bar{u}\mathbf{D}^2 - \bar{u}''\right] \hat{w}, \tag{2.10}$$

$$\lambda \mathbf{D}^2 \hat{u} = \left[\mathbf{D}^4 - Ha^2(\boldsymbol{e}_z \cdot \mathbf{D})^2\right] \hat{u} - \mathbf{D}^2 \left[\mathrm{i}k_x \bar{u}\hat{u} + k_y \bar{u}'\hat{w}\right], \tag{2.11}$$

$$\lambda \hat{T} = \left[Pr^{-1}\mathbf{D}^2 - \mathrm{i}k_x \bar{u}\right] \hat{T} - \bar{T}'\hat{w} + k^{-2}(\mathrm{i}k_x \hat{w}' + k_y \hat{u}), \tag{2.12}$$

where $\mathbf{D} \equiv \left(\boldsymbol{e}_z \mathrm{d}/\mathrm{d}z + \mathrm{i}\boldsymbol{k}\right)$ and the prime denotes derivative with respect to z, $\hat{w} = \boldsymbol{e}_z \cdot \hat{\boldsymbol{v}}$ is the vertical velocity, and $\hat{u} = (\boldsymbol{k} \times \boldsymbol{e}_z) \cdot \hat{\boldsymbol{v}}$ denotes the velocity component perpendicular to the wave vector multiplied by the wavenumber which henceforth is referred to as the longitudinal velocity. Notice that the velocity disturbances are considered in the coordinate system linked with the direction of the wave vector.

The boundary conditions for the vertical velocity $\hat{w}$ are

$$\hat{w}''(\tfrac{1}{2}) + k^2 Re \hat{T}(\tfrac{1}{2}) = 0, \tag{2.13}$$

$$\hat{w}'(-\tfrac{1}{2}) = \hat{w}(\pm\tfrac{1}{2}) = 0. \tag{2.14}$$

For the longitudinal velocity there are two explicit boundary conditions

$$\hat{u}'(\tfrac{1}{2}) = \hat{u}(-\tfrac{1}{2}) = 0. \tag{2.15}$$

Notice that because of the eliminated electrostatic potential the equation for the longitudinal velocity (2.11) has become of the fourth order. Two additional boundary conditions required for $\hat{u}$ follow from the boundary conditions for the induced electric current (2.6). Projecting the linearized Navier–Stokes equation on the vector $\boldsymbol{k} \times \boldsymbol{e}_z$ we obtain the required boundary conditions solely in terms of $\hat{u}$

$$\left[\mathbf{D}^2 - \lambda - Ha^2\right] \hat{u}' - \mathrm{i}k_x \bar{u}'\hat{u} = k_y \bar{u}'\hat{w}' \quad \text{on } z = \pm\tfrac{1}{2}. \tag{2.16}$$

The boundary conditions for the temperature perturbation are

$$\hat{T}'(\tfrac{1}{2}) = 0, \tag{2.17}$$

at the free surface and

$$\hat{T}'(-\tfrac{1}{2}) = 0, \qquad \hat{T}(-\tfrac{1}{2}) = 0 \tag{2.18}$$

at insulating and conducting bottoms, respectively.

For longitudinal disturbances ($k_x = 0$) equations (2.10)–(2.18) can be solved analytically as done by Smith & Davis (1983*a*) for the non-magnetic case. For non-longitudinal disturbances the problem is solved numerically by the modified Chebyshev tau spectral method suggested by Gardner, Trogdon & Douglass (1989).

3. The longitudinal waves

It is instructive to begin the analysis with longitudinal disturbances for which an analytical dispersion relation can be obtained. Although these disturbances are not the most unstable ones, for small Prandtl numbers they may be very close to the most dangerous oblique waves. So analysis of longitudinal waves can be useful for understanding of the more complicated instability mechanism of oblique waves.

The neutral stability curves and the corresponding frequencies calculated from the analytical dispersion relation are shown in figure 2 for $Pr = 0.01$ and various strengths of magnetic field. As is seen, increase of the magnetic field results in the increase of the critical Marangoni number which is given by the global minimum of each neutral

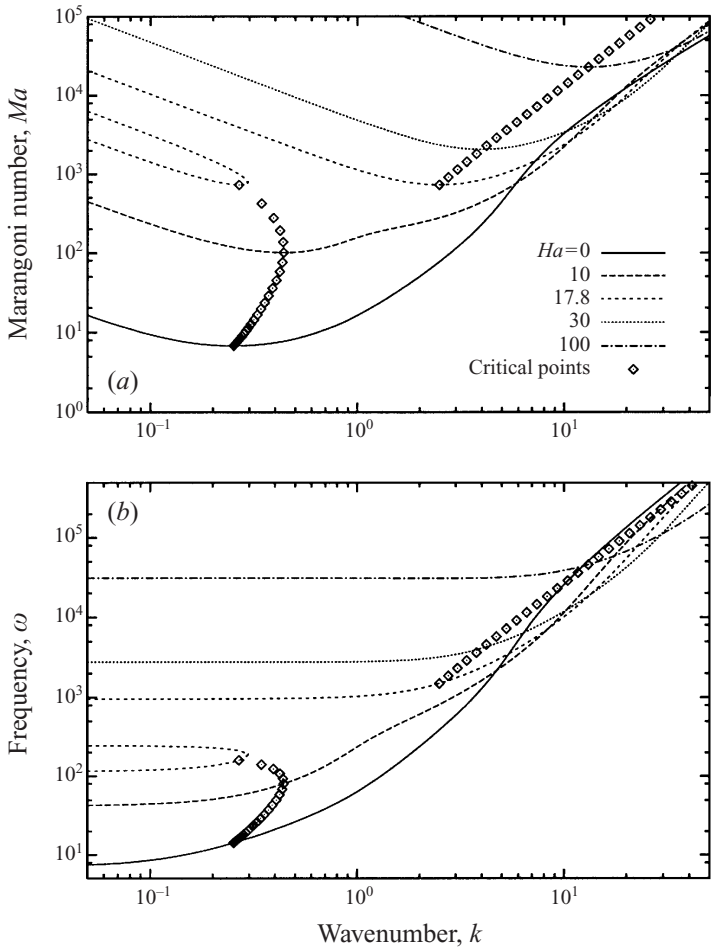

FIGURE 2. The marginal Marangoni number (*a*) and frequency (*b*) of longitudinal mode ($k_x = 0$) versus wavenumber at $Pr = 0.01$ and various Hartmann numbers for an insulating bottom.

curve. The dependence of the instability characteristics on the Hartmann number, which is shown in figure 3, becomes particularly simple in a strong magnetic field ($Ha \gg 1$). In this case, the critical wavenumber increases directly with the Hartmann number meaning that the wavelength of the most dangerous disturbance reduces inversely with the strength of the magnetic field. The critical Marangoni number increases as $\sim Ha^2$. Such asymptotic dependences can straightforwardly be inferred from the effect of the magnetic field on the basic flow which in a strong magnetic field forms a jet at the free surface having the thickness of the Hartmann layer $\sim Ha^{-1}$. This is the effective length scale in the strong magnetic field. Thus the wavenumber, being proportional to the characteristic length, scales as $\sim Ha$ while the Marangoni number and the frequency, being proportional to square of the characteristic length, both scale as $\sim Ha^2$.

3.1. *Hartmann-layer mode*

According to the above considerations, the hydrothermal wave instability in a strong enough magnetic field is due to the jet in the Hartmann layer at the free surface. Therefore it might be useful to focus on the stability of this jet rather than that of

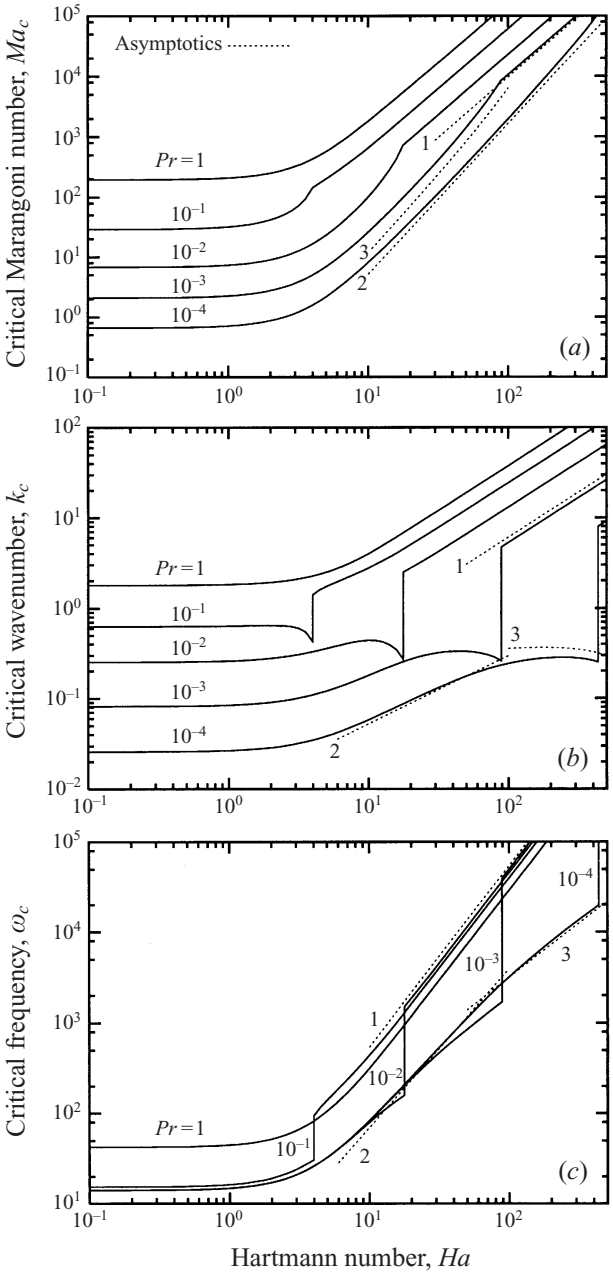

FIGURE 3. The critical Marangoni number (*a*), wavenumber (*b*) and frequency (*c*) of longitudinal waves ($k_x = 0$) versus the Hartmann number at various Prandtl numbers for an insulating bottom. Asymptotics (1), (2) and (3) drawn close to the corresponding numerical results correspond to the Hartmann-layer mode and finite-depth low-frequency and intermediate-frequency modes obtained in §§ 3.1.2, A.1.1 and A.1.2, respectively.

the whole layer. For this purpose, we take the thickness of the Hartmann layer as the characteristic length scale. Then the wavenumber, the frequency and the Reynolds number rescale as

$$k = \tilde{k}Ha, \quad \lambda = \tilde{\lambda}Ha^2, \quad \text{and} \quad Re = \tilde{R}eHa^2. \tag{3.1}$$

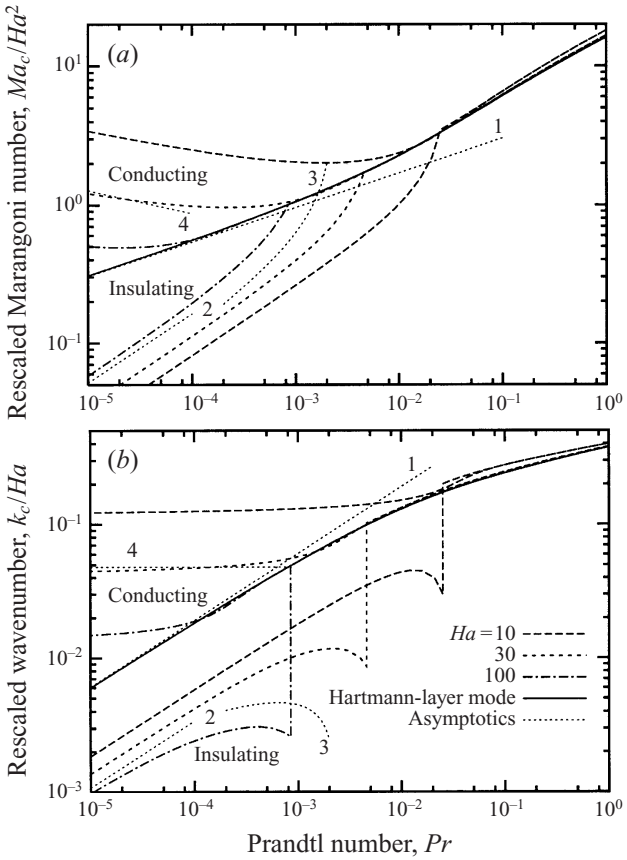

FIGURE 4. The rescaled critical Marangoni number (*a*) and wavenumber (*b*) of longitudinal waves ($k_x = 0$) depending on the Prandtl number at various Hartmann numbers for both insulating and conducting bottoms. Asymptotics (1), (2), (3) and (4), which are close to the corresponding numerical results, correspond to the Hartmann-layer mode and the finite-depth low-frequency and intermediate-frequency modes for an insulating bottom, and finite-depth mode for conducting bottom obtained in §§ 3.1.2, A.1.1, A.1.2 and A.2, respectively.

After rescaling, the leading-order terms of the basic velocity (2.7) and the vertical gradient of temperature profile (2.8) are

$$\tilde{u}(\tilde{z}) = \tilde{R}e\,\mathrm{e}^{-\tilde{z}} \quad \text{and} \quad \tilde{T}'(\tilde{z}) = Pr\,\tilde{R}e(\mathrm{e}^{-\tilde{z}} - 1),$$

where $\tilde{z} = (\frac{1}{2} - z)Ha$. Upon this transformation, equations (2.10)–(2.12) remain mainly unchanged except for the Hartmann number being replaced by unity in equations (2.10), (2.11) and in the boundary conditions (2.16). Finally, rescaling the longitudinal velocity and temperature perturbations by Ha^{-1} and Ha^{-2}, respectively, the stability problem for the Hartmann layer remains explicitly dependent only on the Prandtl number. The critical Marangoni number and wavenumbers calculated from this model along with the exact solution are plotted in figure 4 versus the Prandtl number. For large enough Hartmann numbers both solutions almost coincide thus confirming the validity of the Hartmann-layer model.

3.1.1. *Order-of-magnitude estimates*

The problem can be further simplified by considering the Prandtl number as a small parameter. The advantage of such an approach is twofold. First, it can give a useful insight into particular details of the instability mechanism. Second, it yields simple analytic expressions for the instability parameters. Our goal here is to estimate the marginal Marangoni number together with the associated frequency and, eventually, to locate the minimum of the Marangoni number that gives the threshold of instability. Both the marginal Marangoni number and the corresponding frequency are defined by the balance condition of viscous and thermocapillary stresses at the free surface (2.13) which has to be evaluated from the governing equations. To find both the Marangoni number and the frequency it is necessary to evaluate not only the magnitude of the quantities involved, but also the relative phases of their oscillations. Thus the estimates are carried out in complex form. Moreover, to assess the phase it is necessary to consider not only the leading, but also the next order small contributions (Priede & Gerbeth 1997*b*). The instability mechanism involving interaction of vertical and longitudinal velocity perturbations with the temperature field is, in general, described by Smith (1986). Here we use a non-trivial order-of-magnitude analysis to estimate the critical parameters of this instability.

It is advantageous to begin the analysis with long-wave disturbances. The first necessary quantity is the viscous stress at the free surface which can be estimated as $\hat{w}''(0) \sim (1+\mathrm{i}\tilde{\omega}_0)\hat{w}_0$, where $\tilde{\omega}_0$ is the frequency of marginally stable oscillations to be found and $\hat{w}_0$ is a small but otherwise arbitrary amplitude of the vertical velocity. The real part of the viscous stress, which is in phase with the disturbance of the vertical velocity, is due to the shear over the Hartmann layer. The imaginary part shifted in phase by $\pi/2$ with respect to the real part is due to the viscous oscillatory boundary layer (Priede & Gerbeth 1997*b*). The vertical velocity advecting the non-uniformly distributed momentum of the basic flow further disturbs the longitudinal velocity. The magnitude of this perturbation $\hat{u}_0$ can be estimated by comparing the source term with the sum of viscous and transient terms in equation (2.11) $(1+\mathrm{i}\hat{\omega}_0)\hat{u}_0 \sim \tilde{k}\tilde{R}e\hat{w}_0$. Perturbation of the longitudinal velocity in turn advects the horizontal gradient of the basic temperature field so giving rise to the temperature perturbation. This, occurring in the Hartmann layer at the free surface, diffuses into the bulk of the layer. For the long-wave disturbances, the depth of penetration of the temperature disturbance is determined by the characteristic thickness of the oscillatory thermal boundary layer $\delta_t \sim (\mathrm{i}\tilde{\omega}_0 Pr)^{-1/2}$. To evaluate the temperature perturbation it is advantageous to consider equation (2.12) in an integral form over the depth of the thermal boundary layer which results in

$$|\delta_t|(Pr^{-1}k^2+\mathrm{i}\hat{\omega}_0)\hat{T}_0 \sim \tilde{k}^{-1}\hat{u}_0.$$

So we get rid of the normal gradient of the temperature disturbance which vanishes at both the free surface and outside the thermal boundary layer. The relation obtained states that the heat advected within the Hartmann layer of dimensionless thickness $O(1)$ is all used in transient heating of a layer of thickness $O(\delta_t)$ accompanied by some heat diffusion across the wavelength. The above relations combined with condition (2.13) lead to the following order-of-magnitude analogue of the dispersion relation:

$$(1+\mathrm{i}\hat{\omega}_0)^2(Pr^{-1}\tilde{k}^2+\mathrm{i}\hat{\omega}_0) \sim |\delta_t|^{-1}(\tilde{k}\tilde{R}e)^2. \tag{3.2}$$

Since the right-hand side of the above equation is real, the imaginary part of the left hand side must be zero. This phase balance defines the frequency of neutrally stable

oscillations. For $k \ll 1$, we obtain

$$\tilde{\omega}_0 \sim (1 + 2Pr^{-1}\tilde{k}^2)^{1/2} \sim 1, \tag{3.3}$$

which is very similar to the corresponding result for the case of adiabatic boundaries without magnetic field (Priede & Gerbeth 1997*b*). According to this estimate, the frequency of neutrally stable oscillations is determined by the characteristic viscous diffusion time over the Hartmann layer as long as this time is shorter than the thermal diffusion time over the wavelength. The marginal Reynolds number results from the real part of the dispersion relation (3.2)

$$\tilde{Re} \sim \tilde{k}^{-1}\tilde{\omega}_0|\delta_t|^{1/2} \sim \tilde{k}^{-1}Pr^{-1/4}. \tag{3.4}$$

The marginal Reynolds number decreases with increase of the wavenumber according to the above relation until the thermal diffusion time across the wave becomes as short as the period of neutrally stable oscillations given by the viscous diffusion time over the Hartmann layer. At this point, the thermal diffusion across the wave begins to smooth out the temperature perturbation. As a result, the Reynolds number must increase to maintain the equilibrium between the viscous and thermocapillary stresses at the free surface. This is the effect that selects the critical wavenumber

$$\tilde{k}_c \sim Pr^{1/2}, \tag{3.5}$$

which substituted into (3.4) gives the estimate of the critical Reynolds number

$$\tilde{Re}_c \sim Pr^{-3/4}. \tag{3.6}$$

The validity of the above estimates is confirmed by comparison with the numerical results. Analogously to the case without the magnetic field and adiabatic boundaries (Priede & Gerbeth 1997*b*), estimate (3.5) predicts the critical wavelength to be considerably longer than the characteristic thickness of the Hartmann layer.

3.1.2. *Asymptotic solution*

The estimates obtained allow us to solve the stability problem asymptotically. For this purpose the Reynolds number and wavenumber are rescaled once more in accordance to estimates (3.5), (3.6)

$$\tilde{k} = Pr^{1/2}\check{k}, \quad \tilde{Re} = Pr^{-3/4}\check{Re},$$

and the perturbation amplitudes are expanded in the following asymptotic series of the small parameter $Pr^{1/2}$:

$$\{\hat{w}, \hat{u}, \hat{T}\} = \sum_{n=0}^{\infty} Pr^{n/2}\{Pr^{n/2}w_n, \tilde{k}\tilde{Re}\, u_{n/2}, Pr^{1/2}\tilde{Re}T_{n/2}\}.$$

Equation (2.10) for the leading-order perturbation of the vertical velocity in the Hartmann layer takes the form

$$\frac{\mathrm{d}^2}{\mathrm{d}\tilde{z}^2}\left[\frac{\mathrm{d}^2}{\mathrm{d}\tilde{z}^2} - 1 - \tilde{\lambda}\right] w_0^i = 0, \tag{3.7}$$

whose solution may be written as

$$w_0^i(\tilde{z}) = 1 - \mathrm{e}^{-\gamma_i\tilde{z}}, \tag{3.8}$$

where $\gamma_i = (1+\tilde{\lambda})^{1/2}$. In this case, the perturbation extends outside the Hartmann layer a distance comparable to the wavelength. Therefore we introduce an outer coordinate

$\tilde{z}_o = Pr^{1/2}\tilde{z}$. The leading-order perturbation of the vertical velocity in the bulk of the layer is governed by

$$\left[\frac{\mathrm{d}^2}{\mathrm{d}\tilde{z}_o^2} - \check{k}^2\frac{\tilde{\lambda}}{1+\tilde{\lambda}}\right] w_0^o = 0,$$

whose solution is $w_0^o(\tilde{z}_o) = A_0^o \mathrm{e}^{-z_o\gamma_o}$, where $\gamma_o = \check{k}(\tilde{\lambda}/(1+\tilde{\lambda}))^{1/2}$. Matching of both solutions gives $A_0^o = 1$. The leading-order composite solution asymptotically valid for the whole layer is

$$w_0(\tilde{z}) = w_0^o(\tilde{z}_o) - w_0^o(0) + w_0^i(\tilde{z}) = \exp(-\tilde{z}Pr^{1/2}\gamma_o) - \exp(-\tilde{z}\gamma_i).$$

Now we proceed to the longitudinal velocity whose solution in the bulk of the layer is analogous to the previous one $u_0^o(\tilde{z}_o) = B_0^o \mathrm{e}^{-z_o\gamma_o}$. In the Hartmann layer, equation (2.11) for the leading-order perturbation takes the form

$$\frac{\mathrm{d}^2}{\mathrm{d}\tilde{z}^2}\left[\frac{\mathrm{d}^2}{\mathrm{d}\tilde{z}^2} - 1 - \tilde{\lambda}\right] u_0^i = \frac{\mathrm{d}^2}{\mathrm{d}\tilde{z}^2}(\mathrm{e}^{-\tilde{z}} w_o^i).$$

Upon twofold integration, the above equation transforms into

$$\left[\frac{\mathrm{d}^2}{\mathrm{d}\tilde{z}^2} - 1 - \tilde{\lambda}\right] u_0^i = \mathrm{e}^{-\tilde{z}} w_o^i - (1+\tilde{\lambda})(E_0^i + F_0^i\tilde{z}), \tag{3.9}$$

where E_0^i and F_0^i are constants of integration. Boundedness of the solution implies $F_0^i = 0$. A general solution of this equation is

$$u_0^i(\tilde{z}) = E_0^i + G_0^i \mathrm{e}^{-\tilde{z}\gamma_i} + u_{0,p}^i(\tilde{z}),$$

where

$$u_{0,p}^i(\tilde{z}) = \frac{1}{\gamma_i}\int^{\tilde{z}} \sinh(\gamma_i(\tilde{z}-\tau))\mathrm{e}^{-\tau} w_o^i(\tau)\,\mathrm{d}\tau.$$

The free-slip condition $u_0^{i\prime}(0) = 0$ gives $G_0^i = \gamma_i^{-1} u_{0,p}^{i\prime}(0)$. Because of equation (3.9) the second boundary condition (2.16) is satisfied automatically. Hence the constant E_0^i remains undetermined by the leading-order solution. Matching of the outer and the Hartmann layer solutions yields $B_0^i = E_0^i$. The corresponding composite solution is

$$u_0(\tilde{z}) = u_0^i(\tilde{z}) - E_0^i + u_0^o(\tilde{z}_o).$$

To determine the integration constant E_0^i, we have to consider the next-order perturbation of the longitudinal velocity which is governed by the equation

$$\frac{\mathrm{d}^2}{\mathrm{d}\tilde{z}^2}\left[\frac{\mathrm{d}^2}{\mathrm{d}\tilde{z}^2} - 1 - \tilde{\lambda}\right] u_1^i = \frac{\mathrm{d}^2}{\mathrm{d}\tilde{z}^2}(\mathrm{e}^{-\tilde{z}} w_o^i) + \check{k}^2\left[\frac{\mathrm{d}^2 u_0}{\mathrm{d}\tilde{z}^2} + u_0 - (1+\tilde{\lambda})u_0^o\right]$$

and must satisfy the boundary condition

$$u_1^{i\prime} = \left[\frac{\mathrm{d}^2}{\mathrm{d}\tilde{z}^2} - 1 - \tilde{\lambda}\right] u_1^{i\prime} + \mathrm{e}^{-\tilde{z}} w_1^{i\prime} = 0 \quad \text{on } \tilde{z} = 0.$$

Solvability of this problem imposes an additional constraint resulting from the integration of the above equation over the depth of the layer

$$\int_0^\infty (u_0(\tilde{z}) - (1+\tilde{\lambda})u_0^o(\tilde{z}_o))\,\mathrm{d}\tilde{z} = 0,$$

which yields $E_0^i = Pr^{1/2}E_{1/2}^i$, where $E_{1/2}^i = -\gamma_o\gamma_i/(\tilde{\lambda}(1+\tilde{\lambda})(1+\gamma_i))$. The perturbation of the longitudinal velocity in the bulk of the layer compared to that in the Hartmann

layer is a next-order small quantity $\sim Pr^{1/2}$ which because it occurs over a large depth $\sim Pr^{-1/2}$ advects as much heat as the leading-order perturbation in much thinner Hartmann layer. Thus, for the temperature perturbation, both contributions are equally significant.

For the leading-order temperature perturbation in the outer region equation (2.12) takes the form

$$\left[\frac{\mathrm{d}^2}{\mathrm{d}\tilde{z}_o^2} - \check{k}^2 - \tilde{\lambda}\right] T_0^o = -u_{1/2}^o(\tilde{z}_o),$$

where $u_{1/2}^o(\tilde{z}_o) = Pr^{-1/2} u_0^o(\tilde{z}_o)$. A bounded solution of this equation is

$$T_0^o(\tilde{z}_o) = H_0^o \mathrm{e}^{-\tilde{z}_o \gamma_t} + \theta_0^o(\tilde{z}_o),$$

where

$$\theta_0^o(\tilde{z}_o) = -\frac{1}{\gamma_t} \int^{\tilde{z}_o} \sinh(\gamma_t(\tilde{z}_o - \tau)) u_{1/2}^o(\tau)\, \mathrm{d}\tau.$$

is the particular solution of the non-homogeneous problem and H_0^o is an unknown constant; $\gamma_t = (\check{k}^2 + \tilde{\lambda})^{1/2}$.

In the Hartmann layer, the leading order temperature perturbation is governed by

$$\frac{\mathrm{d}^2 T_0^i}{\mathrm{d}\tilde{z}^2} = -Pr^{1/2} u_0^i(\tilde{z}),$$

whose solution satisfying adiabatic boundary condition $T_0^{i\prime}(0) = 0$ is

$$T_0^i(\tilde{z}) = H_0^i + Pr^{1/2} \theta_0^i(\tilde{z}),$$

where

$$\theta_0^i(\tilde{z}) = -\int_0^{\tilde{z}} (\tilde{z} - \tau) u_0^i(\tau)\, \mathrm{d}\tau.$$

Matching of the bulk and the Hartmann layer temperature perturbations gives $H_0^i = H_0^o + \theta_0^o(0)$. Matching the heat flux leaving the Hartmann layer with that entering the bulk of the layer, we find the last unknown coefficient

$$H_0^o = \frac{1}{\gamma_t}(\theta_0^{o\prime}(0) - \theta_0^{i\prime}(\infty)).$$

Upon substituting the solution found into the stress balance condition (2.13), we obtain the marginal Reynolds number

$$\check{R}e = \check{k}^{-1} \left(-\frac{w_0^{i\prime\prime}(0)}{T_0^i(0)}\right)^{1/2} = \check{k}^{-1} \gamma_i \left(\frac{E_{1/2}^i}{\gamma_t(\gamma_t + \gamma_o)} - \frac{1}{\gamma_t \gamma_i (1 + \gamma_i)}\right)^{-1/2},$$

where the frequency of neutrally stable waves is defined by the equation $\mathrm{Im}[\check{R}e] = 0$ which is to be solved numerically. The marginal Reynolds number and the associated frequency found from the above relations are plotted in figure 5. The minimum of the marginal Reynolds number $\check{R}e_c = 5.4$ is found numerically to occur at the critical wavenumber $\check{k}_c = 1.918$. The corresponding critical frequency is $\tilde{\omega}_c = 5.43$. As is shown in figure 4 (asymptotic 1), this leading-order solution closely approaches that of the Hartmann-layer mode at $Pr \lesssim 10^{-2}$ which is a typical value for liquid metals and semiconductor melts.

Besides, it is seen in figure 4 that at small Prandtl numbers the Hartmann-layer

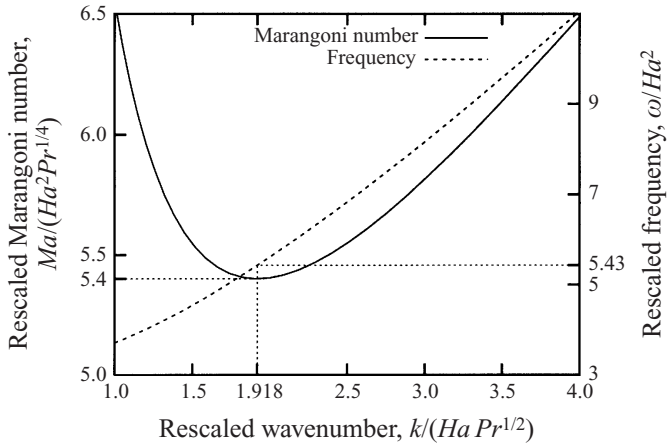

FIGURE 5. Rescaled marginal Marangoni number and rescaled frequency of the longitudinal waves ($k_x = 0$) versus rescaled wavenumber for the Hartmann-layer mode at $Pr \ll 1$.

approximation breaks down leading to results which considerably deviate from the exact solution. The larger the Hartmann number, the smaller the Prandtl number at which the breakdown of the Hartmann-layer approximation occurs. After the breakdown, the instability begins to depend on the thermal properties of the bottom. This happens when the thermal relaxation time over the depth of the layer $\sim Pr$ becomes comparable to the period of oscillations of the Hartmann-layer mode $\sim Ha^{-2}$. Thus the breakdown occurs at $Ha \sim Pr^{-1/2}$ where a transition to an instability mode extending over the whole depth of the liquid layer takes place. Details of this transition depend on the particular thermal boundary conditions at the bottom of the layer. For instance, when the bottom is insulating, the transition proceeds with a jump of the critical wavenumber and frequency (see figures 3 and 4). As is seen in figure 2(a), the jump is related to a pair of local minima developing on the neutral curve with increase of the Hartmann number. At sufficiently high Hartmann numbers, the neutral curve splits into two disconnected branches. At sufficiently small wavenumbers there can be up to three different neutrally stable modes. A jump of the most dangerous instability mode occurs with increase of the Hartmann number as the first local minimum of the neutral curve rises above the second one. For $Pr = 0.01$ plotted in figure 2, this transition occurs at $Ha = 17.8$. Patterns of the critical perturbation for the corresponding instability modes are shown in figure 6. As is seen, besides the wavelength, the principal difference between the two modes is in the distribution of the temperature perturbation over the depth of the layer. With increase of Ha two instability modes merge together and the detached branch vanishes. This will be analysed in detail in the following subsection.

3.2. *Longitudinal finite-depth mode for an insulating bottom*

Outside the range of validity of the Hartmann-layer approximation the instability can also be characterized by certain scaling relations. These relations are obtained directly from the asymptotic solution whose details are presented in the Appendix, § A.1.

According to the numerical results, for an insulating bottom there are two different instability modes extending over the whole depth of the layer. The leading-order asymptotic solution obtained in § A.1.1 for the first one, whose critical frequency is

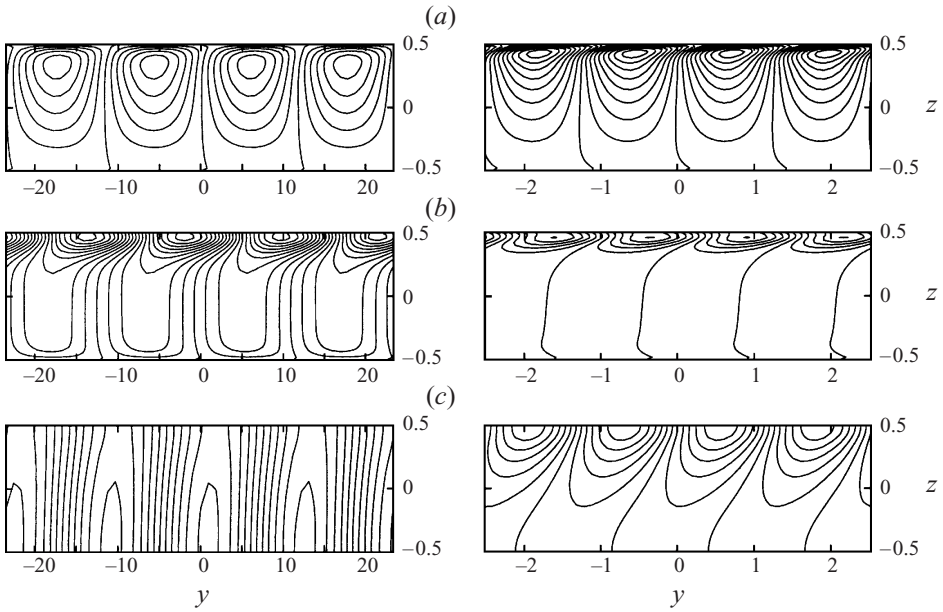

FIGURE 6. Streamlines (*a*), isotachs of longitudinal velocity (*b*) and isotherms (*c*) of the critical longitudinal wave perturbation travelling to the right at $Pr = 0.01$ and $Ha = 17.8$ for low-frequency (left) and intermediate-frequency modes (right).

much lower than the inverse thermal relaxation time over the depth of the layer $\omega \ll Pr^{-1}$, yields the critical wavenumber

$$k_c = \left(\tfrac{4}{3}\right)^{1/4} Pr^{1/2} Ha^{3/4}. \tag{3.10}$$

Note that for $Ha \ll Pr^{-1/2}$ the critical wavelength is much longer than the depth of the layer in accordance with the assumption used to obtain this solution. The leading-order critical frequency and the corresponding Reynolds number defined by equations (A 5) and (A 6) are

$$\omega_c = \tfrac{3}{2} Ha^{7/4}, \qquad Re_c = \left(\frac{8}{3}\frac{Ha^5}{Pr}\right)^{1/2}. \tag{3.11}$$

The above solution (asymptotic 2) together with the exact results are plotted in figures 3 and 4 for $Pr = 10^{-4}$ and $Ha = 100$, respectively. As is seen in figure 4 at small Prandtl numbers, this asymptotic solution closely approaches the corresponding exact solution. However, at larger Prandtl numbers, close to the breakdown of the Hartmann-layer approximation, there is a regular divergence between the asymptotic and exact solutions. This implies that the finite time of thermal relaxation over the depth of the layer, which was neglected in the previous approximation, may be important right after the Hartmann-layer mode breaks down.

The asymptotic solution for this instability mode is obtained in § A.1.2 by assuming the period of neutrally stable oscillations to be considerably shorter than the thermal relaxation time over the whole liquid layer but still much longer than the viscous relaxation time over the Hartmann layer that in terms of frequency is $Pr^{-1} \ll \omega \ll$

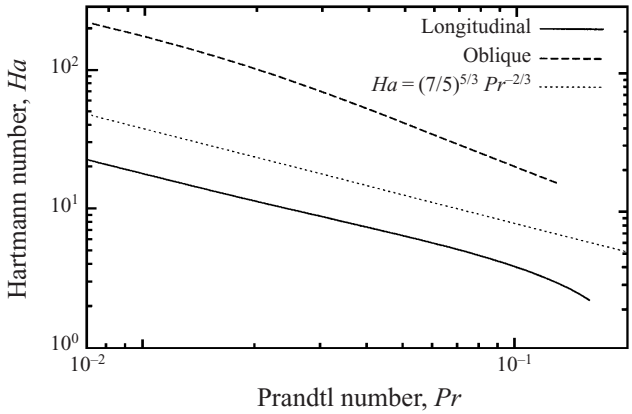

FIGURE 7. Hartmann number at the transition from the finite-depth to the Hartmann-layer instability modes versus the Prandtl number for both longitudinal and oblique waves at adiabatic boundary conditions. The asymptotic solution $Ha = (\frac{7}{5})^{5/3} Pr^{-2/3}$ is obtained in § A.1.2.

Ha^2. The leading-order marginal Reynolds number supplied by this solution is

$$Re \approx \sqrt{2} Ha^{3/2} \frac{\omega}{k} = \sqrt{2} Ha^{5/2} Pr^{-1/2} \left(\frac{7}{4} - \left(\frac{Pr\,\omega}{2} \right)^{1/2} - Ha^3\, \omega^{-2} \right)^{-1/2}. \tag{3.12}$$

The critical frequency ω_c, at which the marginal Reynolds number attains its minimum, is defined by $\mathrm{d}Re/\mathrm{d}\omega = 0$ yielding

$$\omega_c = 2 \left(\frac{Ha^6}{Pr} \right)^{1/5}. \tag{3.13}$$

As is seen in figure 3(c) (asymptotic 3), the above result is not only in qualitative, but also in surprisingly good quantitative agreement with the exact solution. In contrast to this, for the critical Reynolds number and wavenumber defined by equations (A 8) and (3.12) there are noticeable offsets between the exact and asymptotic solutions seen in figures 3(a, b) and 4(a, b) (asymptotic 3). Despite the offset, the asymptotic solution clearly reproduces the principal feature of the exact solution, namely the singularity of the critical wavenumber and the Reynolds number developing at $Ha \sim Pr^{-2/3}$. At this point, the critical wavenumber tends to zero while the Reynolds number goes to infinity. So the finite-depth instability disappears and the most dangerous instability switches to the Hartmann-layer mode.

Although the previous results suggest that for sufficiently small Prandtl numbers this transition occurs at $Ha \sim Pr^{-1/2}$, for moderately small Pr the scaling of the Hartmann number at which the transition takes place is very close to $\sim Pr^{-2/3}$ (see figure 7). It may be seen in figure 4(a, b) that the effect of the singularity diminishes with decrease of the Prandtl number. As a result, direct transition from the Hartmann-layer to the low-frequency mode, which can be estimated by comparing the corresponding critical Reynolds numbers to occur at $Ha_2 = 10.9 Pr^{-1/2}$, takes place when $Ha_* \gtrsim Ha_2$. Thus the small-Prandtl-number scaling is anticipated at $Pr \lesssim 10^{-5}$ which is far too small to be of practical significance.

3.3. *Longitudinal finite-depth mode for a conducting bottom*

The bottom of the layer is expected to begin to affect the instability occurring at the free surface when the characteristic thermal relaxation time over the depth of the layer becomes comparable to the period of oscillations. According to the Hartmann-layer model considered above, this happens at sufficiently small Prandtl numbers $Pr \sim Ha^{-2}$. Note that at this point the critical wavelength of the Hartmann-layer mode becomes comparable to the depth of the layer $k_c \sim 1$. According to equation (2.12), at wavelengths larger than the layer depth, the temperature disturbance is dominated by the vertical heat flux over the depth of the layer. The latter being independent of the wavelength leads to the magnitude of the temperature perturbation being such as well. This results in a critical wavelength comparable to the layer depth as it does for the corresponding case without a magnetic field (Priede & Gerbeth 1997*b*). Scalings of the Marangoni number and the associated frequency can be estimated from the following order-of-magnitude considerations which will be carried out in terms of the Hartmann-layer variables.

The thermal relaxation time over the depth of layer becoming shorter than the viscous relaxation time of the Hartmann layer leads to an increase of the frequency of neutrally stable oscillations. So the frequency becomes larger than the inverse viscous relaxation time over the Hartmann layer. Similarly to when there is no magnetic field, this leads to the development of an oscillatory boundary layer of thickness $\tilde{\omega}^{-1/2}$ within the Hartmann layer at the free surface. As a result, the shear stress at the free surface becomes dominated by the oscillatory boundary layer rather than the Hartmann layer $\hat{w}''(0) \sim \mathrm{i}\hat{w}_0$. Perturbation of the longitudinal velocity in the Hartmann layer is determined by the balance of inertia on one side and advection of momentum of the basic flow by perturbation of the vertical velocity on the other side $\mathrm{i}\tilde{\omega}_0\hat{u}_0 \sim \tilde{R}e\hat{w}_0$. Perturbation of the longitudinal velocity in the oscillatory boundary layer, which is driven by shear stress due to the flow in the Hartmann layer, has the same order of magnitude as in the Hartmann layer. However, the inertia of the viscous boundary layer causes this perturbation to be delayed in phase by $\pi/2$, i.e., $\mathrm{i}\hat{u}_1 \sim \hat{u}_0$ (Priede & Gerbeth 1997*b*). The last relation needed to define the magnitude of the temperature perturbation is obtained by considering equation (2.12) in the integral over the depth of the layer

$$(Ha^{-2}Pr^{-1} + \mathrm{i}\tilde{\omega}_0)\hat{T}_0 \sim Ha^{-1}(\hat{u}_0 + \tilde{\omega}_0^{-1/2}\hat{u}_1).$$

Combination of the relations obtained above leads to the following order-of-magnitude analogue of the dispersion relation:

$$\tilde{\omega}_0^2(1 + \mathrm{i}\tilde{\omega}_0^{-1/2})(Ha^{-2}Pr^{-1} + \mathrm{i}\tilde{\omega}_0) \sim Ha^{-3}\tilde{R}e^2.$$

The imaginary part of the dispersion relation gives the frequency of neutrally stable waves in the original dimensionless terms as $\omega_0 \sim (Ha/Pr)^{2/3}$. The corresponding critical Reynolds number resulting from the real part of the above dispersion relation is $Re_c \sim (Ha/Pr)^{7/6}$. This estimate suggests that, in contrast to the case of adiabatic boundaries, the critical Marangoni number increases slower with the Hartmann number in the finite-depth mode than in the Hartmann-layer mode. Note that the dependence of the critical parameters on the Prandtl number is the same as without the magnetic field (Priede & Gerbeth 1997*b*).

The corresponding asymptotic solution, whose details are given in the Appendix, § A.2, yields the critical Reynolds number $Re_c = 3.18(Ha/Pr)^{7/6}$ occurring at the critical wavenumber $k_c = 1.44$. The corresponding frequency is $\omega_c = 3.62(Ha/Pr)^{2/3}$. The critical Marangoni number and wavenumber are seen in figures 4(*a*) and 4(*b*)

(asymptotic 4) to be close to the corresponding numerical results, which confirms the accuracy of the asymptotic solution found.

4. The oblique waves

Like the case without a magnetic field, for small-Prandtl-number liquids the most unstable disturbances are not strictly longitudinal, but rather slightly oblique. Numerically found critical Marangoni numbers and the angles between the x-axis and the wave vectors of the most unstable oblique waves for various Prandtl numbers are plotted in figures 8(a) and 8(b) versus the Hartmann number. As is seen, increase of the magnetic field results in a monotonic increase of the critical Marangoni number. As for the longitudinal waves, in a sufficiently strong magnetic field the instability ceases to depend on the thermal properties of the bottom, and the critical Marangoni number becomes $\sim Ha^2$. As discussed above, this is due to the instability of the Hartmann layer at the free surface. To investigate this instability mode in more detail it is useful to rescale all the variables by taking the thickness of the Hartmann layer as the characteristic length scale as was done for longitudinal waves above. The advantage of the rescaling is in the elimination of the Hartmann number from the rescaled problem which remains dependent only on the Prandtl number. Note that the magnitude of the Hartmann number necessary for validity of this approximation depends on the Prandtl number. The rescaled problem like the original one is solved numerically with the difference that now the layer is treated as effectively unbounded in depth.

The rescaled critical parameters of the most unstable oblique wave along with those supplied by the Hartmann-layer approximation are plotted versus the Prandtl number in figure 9. With increase of the Hartmann number the exact solution clearly approaches the Hartmann-layer mode. As expected, development of the Hartmann-layer mode depends not only on the Hartmann number, but also on the Prandtl number. The smaller the Prandtl number, the higher the Hartmann number at which the Hartmann-layer mode becomes the most dangerous one. For sufficiently small Prandtl number the most dangerous instability mode depends on the thermal properties of the bottom. As for longitudinal waves, the breakdown of the Hartmann-layer mode proceeds with a jump of the critical wave vector and frequency when the bottom of the layer is thermally insulating. The transition in the most unstable mode is continuous when the bottom is a good conductor. In contrast to the longitudinal waves, now the Hartmann number necessary for the Hartmann-layer mode to be the most dangerous one is about an order of magnitude larger (see figure 7a).

4.1. *Small-Prandtl-number asymptotics of the Hartmann-layer mode*

The Hartmann-layer approximation can be further simplified by considering the Prandtl number to be small. Actually, the Prandtl numbers for liquid metals or molten semiconductors are indeed small $\sim 10^{-2}$. This fact can be employed to solve the problem asymptotically similarly to that for the longitudinal waves. Such an approach is expected to yield simple expressions for the critical parameters applicable at sufficiently small Prandtl and large Hartmann numbers. Once the asymptotic solutions are found, their range of validity can be estimated.

There are two important facts of use in the asymptotic analysis suggested by the numerical solution. First, at small Prandtl numbers the critical wavelength of oblique disturbances is considerably longer than the thickness of the Hartmann layer, implying $\tilde{k} \ll 1$. Second, the frequency of neutrally stable waves is comparable to

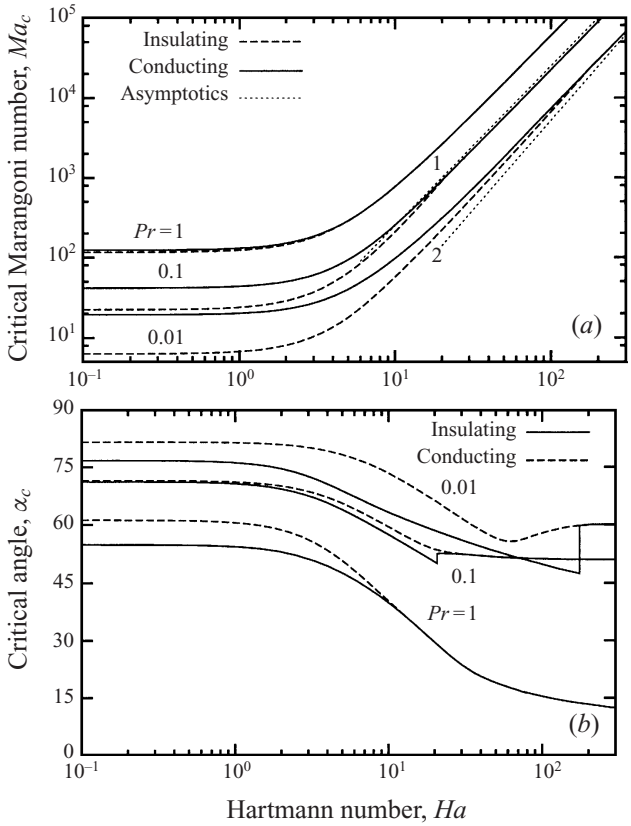

FIGURE 8. Critical Marangoni number (*a*) and the angle between the direction of the *x*-axis and the wave vector of the most unstable oblique wave (*b*) versus the Hartmann number at various Prandtl numbers. Asymptotics (1) $Ma_c = 7.86Pr^{1/2}Ha^2$ and (2) $Ma_c = 1.64Pr^{1/2}Ha^{9/4}$ correspond to the Hartmann-layer and the finite-depth modes considered in §§ 4.1 and 4.2, respectively.

the inverse diffusion time over the wavelength $\omega \sim k^2$. In contrast to the case of the longitudinal waves, the frequency is much lower than the inverse viscous relaxation time over the thickness of the Hartmann layer.

The perturbation amplitudes are sought as

$$\{\hat{w}, \hat{u}, \hat{T}\} = \sum_{n=0}^{\infty} \varepsilon_n \{w_n, \tilde{k}_y \tilde{Re}\, u_n, \tilde{k}^{-2} Pr\, \tilde{Re} T_n\},$$

where $\varepsilon_0 = 1$ while ε_n, for $n \geqslant 1$ is an unknown asymptotic series to be found in the course of the solution. Considering $k^2 \ll 1$, equation (2.10) for the leading-order disturbance of the vertical velocity in the Hartmann layer takes the form

$$\left[\frac{\mathrm{d}^2}{\mathrm{d}\tilde{z}^2} - \mathrm{i}\tilde{k}_x \tilde{Re}\, \mathrm{e}^{-z}\right]\left[\frac{\mathrm{d}^2}{\mathrm{d}\tilde{z}^2} - 1\right] w_0^i = 0, \tag{4.1}$$

where $\tilde{Re}$ and $\tilde{k}$ are Reynolds number and wavenumber based on the characteristic thickness of the Hartmann layer. Because in the framework of linear stability analysis the amplitude of the disturbance is defined up to an arbitrary factor, the temperature perturbation of the free surface may be rescaled so that the stress balance condition

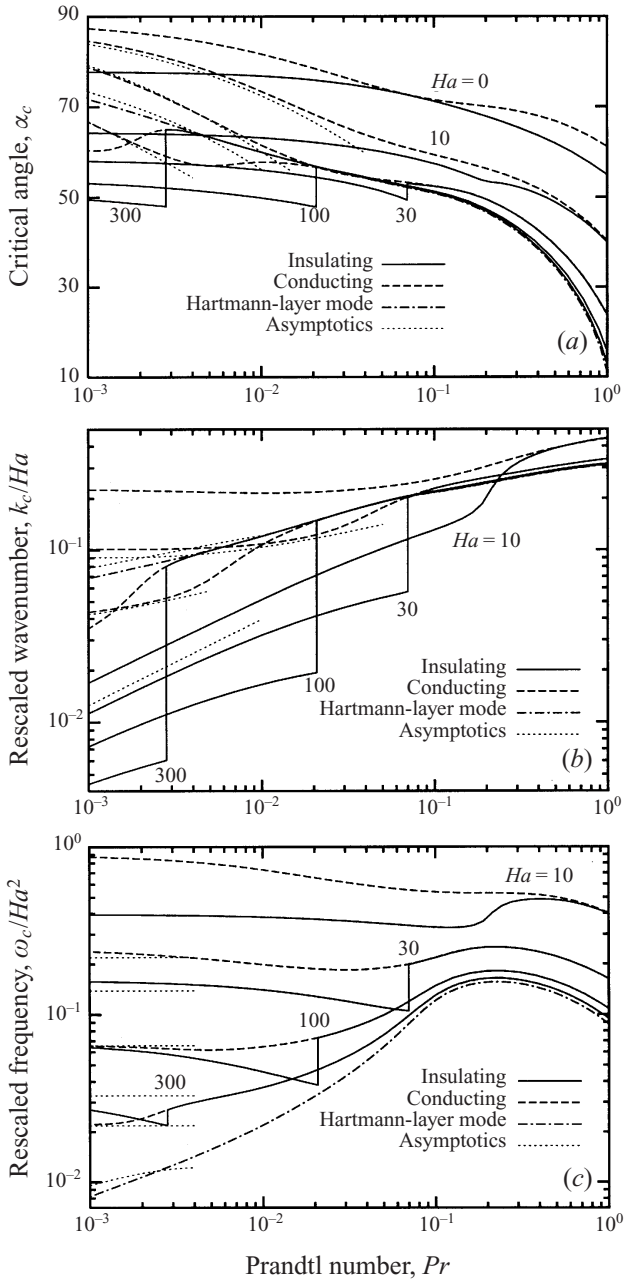

FIGURE 9. The angle between the x-axis and the wave vector of the most unstable oblique wave (a), the rescaled critical wavenumber (b), and frequency (c) versus the Prandtl number at various Hartmann numbers. Asymptotics are plotted close to the corresponding numerical results.

(2.13) takes the form

$$w_0^{i\prime\prime}(0) = 1, \tag{4.2}$$

whereas the other boundary condition is $w_0^i(0) = 0$. Although the above problem admits an analytic solution involving integrals of the Bessel functions, we solve it

numerically by a tau spectral method employing Chebyshev polynomials with an exponential mapping of the semi-infinite interval (Canuto *et al.* 1988).

Comparing the terms dominating in equations (2.10), (2.11) outside the Hartmann layer, it follows that disturbances extend into the underlying liquid up to the distance proportional to the square of their wavelength $\sim \tilde{k}^{-2}$. This is the range at which disturbances with a characteristic width across the magnetic flux lines increasing as square root of the distance along the flux lines merge together and thus smooth out. Outside the Hartmann layer, we introduce a contracted outer coordinate: $\tilde{z}_o = \tilde{k}^2\tilde{z}$ in terms of which equation (2.10) takes the form

$$\left[\frac{\mathrm{d}^2}{\mathrm{d}\tilde{z}_o^2} - 1 - \check{\lambda}\right] w_0^o = 0,$$

where

$$\check{\lambda} = \tilde{\lambda}/\tilde{k}^2 \tag{4.3}$$

is the rescaled frequency. The bounded solution of this equation matching the Hartmann layer solution may be written as $w_0^o(\tilde{z}_o) = w_0^i(\infty)\mathrm{e}^{-\tilde{z}_o\gamma_o}$. The composite leading-order solution valid in the whole layer may be constructed as $w_0(\tilde{z}) = w_0^i(\tilde{z}) + w_0^o(\tilde{z}_o) - w_0^i(\infty)$.

Now we can proceed to the leading-order solution for the perturbation of the longitudinal velocity. To simplify the matching of the solution it is advantageous to rewrite equation (2.11) as a system of two equations involving the vertical component of the induced current $\hat{j}$ (Priede & Gerbeth 1997*a*):

$$\left[\mathbf{D}^2 - \lambda\right]\hat{u} - \mathrm{i}k_x\bar{u}\hat{u} - k_y\bar{u}'\hat{w} + \mathrm{i}Ha(\boldsymbol{e}_z\cdot\mathbf{D})\hat{j} = 0, \tag{4.4}$$

$$\mathrm{i}Ha(\boldsymbol{e}_z\cdot\mathbf{D})\hat{u} = \mathbf{D}^2\hat{j}. \tag{4.5}$$

Use of $\hat{j}$ in matching Hartmann-layer and outer-region solutions allows us to find a unique leading-order solution without resorting to the solvability conditions for the higher-order approximations as it was necessary above. Besides, it is advantageous to divide the solution into the Hartmann-layer contribution $u_0^i(\tilde{z})$ and outer-region one $u_n^o(\tilde{z}_o)$:

$$u_n = u_n^i(\tilde{z}) + u_n^o(\tilde{z}_o).$$

This partition is uniquely defined by requiring $u_n^i(\infty) = 0$. For the Hartmann layer, equation (4.5) takes the form

$$\frac{\mathrm{d}^2 j_0^i}{\mathrm{d}\tilde{z}^2} = -\mathrm{i}\frac{\mathrm{d}u_0^i}{\mathrm{d}\tilde{z}},$$

whose solution satisfying the boundary condition $j_0^i(0) = 0$ is

$$j_0^i(\tilde{z}) = -\mathrm{i}\int_0^{\tilde{z}} (u_0^i(\tau) - E_0^i)\,\mathrm{d}\tau, \tag{4.6}$$

where E_0^i is an unknown constant to be determined from the boundary conditions for u_0^i. Upon substitution of the above solution into equation (4.4), we obtain for the leading-order perturbation in the Hartmann layer

$$\left[\frac{\mathrm{d}^2}{\mathrm{d}\tilde{z}^2} - 1\right] u_0^i - \mathrm{i}k_x\tilde{R}e\,\mathrm{e}^{-\tilde{z}}(u_0^i(\tilde{z}) + u_0^o(0)) = \mathrm{e}^{-\tilde{z}}w_0^i - E_0^i. \tag{4.7}$$

The condition $u_n^i(\infty) = 0$ applied to this equation yields $E_0^i = 0$. To solve the above

equation we need first to define $u_0^o(0)$ in terms of u_0^i. This can be done by considering the outer region where equations (4.4), (4.5) take the form

$$(1+\tilde{\lambda})u_0^o + \mathrm{i}\frac{\mathrm{d}\, j_0^o}{\mathrm{d}\tilde{z}_o} = 0, \tag{4.8}$$

$$j_0^o - \mathrm{i}\frac{\mathrm{d}u_0^o}{\mathrm{d}\tilde{z}_o} = 0. \tag{4.9}$$

The bounded solution for the longitudinal velocity is found as $u_0^o(\tilde{z}_o) = B_0^o \mathrm{e}^{-\gamma_o \tilde{z}}$. Matching of the electric current between the outer region and the Hartmann layer, defined by equations (4.9), (4.6), respectively, yields the relation

$$B_0^o = \gamma_o^{-1} \int_0^\infty u_0^i(\tilde{z})\, \mathrm{d}\tilde{z}, \tag{4.10}$$

which allows us to eliminate $u_0^o(0) = B_0^o$ from the equation (4.7) and thus to complete the formulation of the problem for perturbation of the longitudinal velocity in the Hartmann layer:

$$\left[\frac{\mathrm{d}^2}{\mathrm{d}\tilde{z}^2} - 1\right] u_0^i - \mathrm{i}k_x \tilde{R}e\, \mathrm{e}^{-\tilde{z}} \left[u_0^i(\tilde{z}) + \gamma_o^{-1} \int_0^\infty u_0^i(\tilde{z})\, \mathrm{d}\tilde{z}\right] = -\mathrm{e}^{-\tilde{z}} w_0^i. \tag{4.11}$$

Solution of this integro-differential equation satisfying the boundary condition $u_0^{i\prime}(0) = 0$ is found numerically like that of equation (4.1).

Now it remains to find the leading-order temperature perturbation for which equation (2.12) in the Hartmann layer takes the form $\mathrm{d}^2 T_0^i/\mathrm{d}\tilde{z}^2 = 0$. The bounded solution of this equation satisfying the adiabatic boundary condition at the free surface is constant: $T_0^i(\tilde{z}) = C_0^i$. In the outer region, the temperature disturbance is determined only by heat diffusion. It means that the characteristic distance of variation of temperature is comparable to the wavelength of the disturbance. Therefore, to find the distribution of the temperature disturbance in the outer region it is useful to introduce another contracted coordinate $\tilde{z}_t = k\tilde{z}$, in terms of which equation (2.12) for the leading-order temperature perturbation takes the form

$$\left[\frac{\mathrm{d}^2}{\mathrm{d}\tilde{z}_t^2} - 1\right] T_0^o = -B_0^o \sin^2(\alpha),$$

A solution of this equation matching with that of the Hartmann layer is $T_0^o(\tilde{z}) = B_0^o \sin^2(\alpha)$. Substituting this solution into the stress balance condition (2.13) and taking into account the additionally imposed scaling condition (4.2) we obtain

$$Pr\, \tilde{R}e^2 B_0^o \sin^2(\alpha) - 1 = 0. \tag{4.12}$$

This is a complex equation defining the leading-order marginal Reynolds number and the frequency of neutrally stable waves as function of wavenumber k and the direction of the wave vector with respect to the x-axis specified by the angle α. The critical Reynolds number at which the first neutrally stable disturbance appears is given by a minimum value of the marginal Reynolds number. Before proceeding to the solution of the above equation it is worth noting that both the Prandtl number and the angle α can be eliminated from the set of equations (4.1), (4.11), and (4.12) by rescaling the Reynolds number and streamwise wavenumber as

$$\tilde{R}e = \check{R}e/(Pr^{1/2} \sin(\alpha)), \tag{4.13}$$

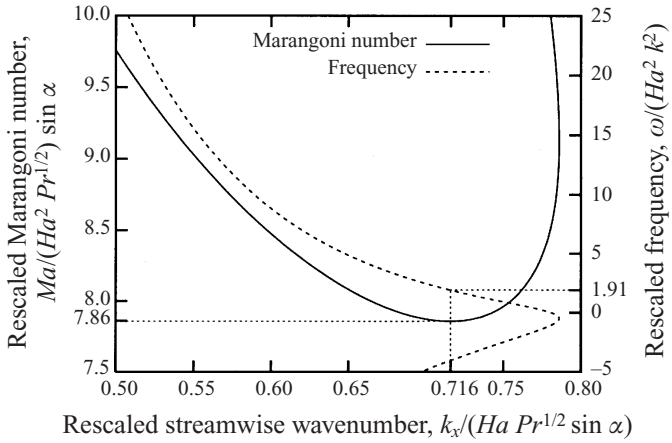

FIGURE 10. Leading-order rescaled marginal Marangoni number and rescaled frequency of the oblique wave mode versus rescaled streamwise wavenumber for the Hartmann-layer instability at $Pr \ll 1$.

$$\tilde{k}_x = \check{k}_x Pr^{1/2} \sin(\alpha). \tag{4.14}$$

Thus $\check{R}e$ is a function only of $\check{k}_x$. Then it follows from equation (4.13) that the leading-order marginal Reynolds number attains its minimum at $\alpha_c = \pi/2$. It means that with a decrease of the Prandtl number the most dangerous oblique waves tend to become almost longitudinal. The corresponding leading order critical Reynolds number and corresponding streamwise wavenumber are

$$\tilde{R}e_c = Pr^{-1/2}\check{R}e_c, \qquad \tilde{k}_{x,c} = Pr^{1/2}\check{k}_{x,c}.$$

The leading-order rescaled marginal Reynolds number and the corresponding frequency versus the rescaled streamwise wavenumber are plotted in figure 10. According to this solution the critical rescaled Reynolds number $\check{R}e_c = 7.86$ is attained at $\check{k}_{x,c} = 0.716$. The corresponding rescaled frequency is $\check{\omega} = 1.91$. It may be seen in figure 8(*a*) that the above solution (asymptotic 1) closely approaches the corresponding critical Marangoni number for such moderate values as $Ha \gtrsim 10$ and $Pr \lesssim 0.1$.

Note that the leading-order solution obtained above gives only the streamwise component of the critical wave vector while the magnitude and the direction of the wave vector are left undetermined. The same holds also for the critical frequency defined through the wavenumber by equation (4.3). To determine the critical wavenumber it is necessary to consider the next order asymptotic solution. For this purpose first we need to assess its order of magnitude. The next-order correction will partly be due to the terms $\sim \tilde{k}^2$ which were neglected in equations (2.10) and (2.11) in obtaining the leading-order solution. Note that this correction is related to the reduction of the wavelength as $\alpha \to \pi/2$ while the streamwise wavenumber remains fixed. This effect is expected to cause an increase of the marginal Reynolds number by $\sim \tilde{k}^2\tilde{R}e \sim \tilde{k}_x^2\tilde{\alpha}^{-2}\tilde{R}e$, where $\tilde{\alpha} = \pi/2 - \alpha$. On the other hand, it follows from equation (4.13) that the leading-order marginal Reynolds number decreases by $\sim \tilde{\alpha}^2\tilde{R}e$ as the oblique mode approaches the longitudinal one. Consequently, increment of the marginal Reynolds number due to both effects will be minimal at $\tilde{\alpha}^2 \sim \tilde{k}_x^2\tilde{\alpha}^{-2}$ yielding

$$\tilde{\alpha}_c \sim \tilde{k}_x^{1/2} \sim Pr^{1/4} \quad \text{and} \quad \tilde{k}_c \sim \tilde{k}_x/\tilde{\alpha}_c \sim Pr^{1/4}.$$

To find the next-order correction $\sim \varepsilon_1 \sim \tilde{k}^2 \sim Pr^{1/2}$ we rescale the wavenumber

and the angle in accordance with the above estimates as $\tilde{k} = Pr^{1/4}\check{k}$ and $\alpha = \pi/2 - Pr^{1/4}\check{\alpha}$, respectively, and expand the Reynolds number and frequency as $\{\check{R}e, \check{\lambda}\} = \sum_{n=0}^{\infty} \varepsilon_n \{\check{R}e_n, \check{\lambda}_n\}$. Then equation (2.10) for the first order correction of the vertical velocity in the Hartmann layer takes the form

$$\left[\frac{\mathrm{d}^2}{\mathrm{d}\tilde{z}^2} - \mathrm{i}\check{k}_{0,x}\check{R}e_0\mathrm{e}^{-z}\right]\left[\frac{\mathrm{d}^2}{\mathrm{d}\tilde{z}^2} - 1\right] w_1^i = \check{k}^2((2+\check{\lambda}_0)\frac{\mathrm{d}^2 w_0^i}{\mathrm{d}\tilde{z}^2} - \mathrm{i}\check{k}_{0,x}\check{R}e_0\mathrm{e}^{-z}(w_0^i(\tilde{z}) + \tilde{z}w_0^{o\prime}(0))) + \mathrm{i}\check{k}_{0,x}\check{R}e_1\mathrm{e}^{-z}\left[\frac{\mathrm{d}^2}{\mathrm{d}\tilde{z}^2} - 1\right] w_0^i, \quad (4.15)$$

whereas the boundary conditions are $w_1^i(0) = w_1^{i\prime\prime}(0) = 0$. In the outer region, the corresponding equation is

$$\left[\frac{\mathrm{d}^2}{\mathrm{d}\tilde{z}_o^2} - 1 - \check{\lambda}\right] w_1^o = -(2+\check{\lambda}_0)(1+\check{\lambda})w_0^o(\tilde{z}_o),$$

whose solution matching the Hartmann layer perturbation is

$$w_1^o(\tilde{z}_o) = (w_1^i(\infty) + \tilde{z}_o w_0^i(\infty)(2+\check{\lambda}_0)(1+\check{\lambda})/(2\gamma_o))\mathrm{e}^{-\gamma_o\tilde{z}_o}.$$

Having found the first-order perturbation of the vertical velocity, we use it further to obtain the corresponding solution for the longitudinal velocity. Equation (4.5) for the first-order perturbation in the Hartmann layer takes the form

$$\frac{\mathrm{d}^2 j_1^i}{\mathrm{d}\tilde{z}^2} = -\mathrm{i}\frac{\mathrm{d}u_1^i}{\mathrm{d}\tilde{z}} + j_0^i(\tilde{z}) - j_0^i(\infty),$$

whose bounded solution satisfying $j_1^i(0) = 0$ can be obtained as

$$j_1^i(\tilde{z}) = -\mathrm{i}\int_0^{\tilde{z}} (u_1^i(\tau) - E_1^i)\,\mathrm{d}\tau + \int_0^{\tilde{z}}\int_\infty^\tau (j_0^i(\xi) - j_0^i(\infty))\,\mathrm{d}\xi\,\mathrm{d}\tau. \quad (4.16)$$

As for the analogous leading-order solution considered above, the condition $u_1^i(\infty) = 0$ implies $E_1^i = 0$. Equations (2.11) and (4.5) for the first-order corrections in the outer region are

$$(1+\check{\lambda}_0)u_1^o + \mathrm{i}\frac{\mathrm{d}j_1^o}{\mathrm{d}\tilde{z}_o} = \check{k}^2\frac{\mathrm{d}^2 u_0^o}{\mathrm{d}\tilde{z}_o^2} - \check{\lambda}_1 u_0^o(\tilde{z}_o), \quad (4.17)$$

$$j_1^o - \mathrm{i}\frac{\mathrm{d}u_1^o}{\mathrm{d}\tilde{z}_o} = \check{k}^2\frac{\mathrm{d}^2 j_0^o}{\mathrm{d}\tilde{z}_o^2}. \quad (4.18)$$

The solution of these equations for the longitudinal velocity correction may be written as

$$u_1^o(\tilde{z}_o) = (B_1^o + \tilde{z}_o B_0^o(\check{k}^2(2+\check{\lambda}_0)(1+\check{\lambda}_0) - \check{\lambda}_1)/(2\gamma_o))\mathrm{e}^{-\gamma_o\tilde{z}_o}.$$

Matching the vertical electric current correction in the outer region with that in the Hartmann layer defined by equations (4.18) and (4.16), respectively, we obtain

$$B_1^o = \gamma_o^{-1}\int_0^\infty (u_1^i(\tilde{z}) - \mathrm{i}\check{k}^2\tilde{z}(j_0^i(\tilde{z}) - j_0^i(\infty)))\,\mathrm{d}\tilde{z} - \frac{B_0^o}{2}\left(\check{k}^2\check{\lambda}_0 + \frac{\check{\lambda}_1}{1+\check{\lambda}_0}\right).$$

Substituting solution (4.16) into equation (2.11) and making use of the above relation we obtain the following equation for the first-order correction of the longitudinal

velocity in the Hartmann layer

$$\left[\frac{\mathrm{d}^2}{\mathrm{d}\tilde{z}^2}-1\right]u_1^i-\mathrm{i}\check{k}_x\check{R}e\,\mathrm{e}^{-\tilde{z}}\left[u_1^i(\tilde{z})+\gamma_o^{-1}\int_0^\infty u_1^i(\tilde{z})\,\mathrm{d}\tilde{z}\right]$$
$$=\check{k}^2(\mathrm{e}^{-\tilde{z}}(w_1^i(\tilde{z})+\tilde{z}w_0^{o\prime}(0))+\mathrm{i}\int_\infty^{\tilde{z}}(j_0^i(\tau)-j_0^i(\infty))\,\mathrm{d}\tau+(1+\check{\lambda}_0)u_0^i(\tilde{z}))$$
$$-\mathrm{i}\check{k}_{0,x}\check{R}e_0\mathrm{e}^{-\tilde{z}}\left(\mathrm{i}\check{k}^2\gamma_o^{-1}\int_0^\infty\tilde{z}(j_0^i(\tilde{z})-j_0^i(\infty))\,\mathrm{d}\tilde{z}-\check{k}^2\tilde{z}u_0^{o\prime}(0)\right.$$
$$\left.+\frac{B_0^o}{2}\left(\check{k}^2\check{\lambda}_0+\frac{\check{\lambda}_1}{1+\check{\lambda}_0}\right)\right)+\mathrm{i}\check{k}_{0,x}\check{R}e_1\mathrm{e}^{-\tilde{z}}(u_0^i(\tilde{z})+B_0^o). \tag{4.19}$$

The corresponding boundary condition takes the form $u_1^{i\prime}(0)=\check{k}^2\gamma_oB_0^o$. This completes the formulation of the problem for the first-order perturbation of the longitudinal velocity which is solved numerically.

Now we can proceed to the first order temperature perturbation governed in the Hartmann layer by

$$\frac{\mathrm{d}^2T_1^i}{\mathrm{d}\tilde{z}^2}=-\check{k}^2u_0^i(\tilde{z})+\mathrm{i}Pr^{1/2}\check{k}_{0,x}(\check{R}e_0Pr\,\mathrm{e}^{-\tilde{z}}B_0^o+\check{R}e_0^{-1}w_0^{i\prime}(\tilde{z})).$$

The solution of this equation satisfying the adiabatic boundary condition $T_1^{i\prime}(0)=0$ is

$$T_1^i(\tilde{z})=C_1^i-\int_0^{\tilde{z}}(z-\tau)(\check{k}^2u_0^i(\tau)-\mathrm{i}Pr^{1/2}\check{k}_{0,x}(\check{R}e_0Pr\,\mathrm{e}^{-\tau}B_0^o+\check{R}e_0^{-1}w_0^{i\prime}(\tau))\,\mathrm{d}\tau,$$

where C_1^i is an unknown constant to be determined by matching the Hartmann layer and outer region solutions. In the outer region, the temperature perturbation is governed by

$$\left[\frac{\mathrm{d}^2}{\mathrm{d}\tilde{z}_t^2}-1\right]T_1^o=-B_1^o+\check{k}^2B_0^o\tilde{z}.$$

A bounded solution of the above equation may be written as

$$T_1^o(\tilde{z})=C_1^o\exp(-Pr^{1/4}\check{k}\tilde{z})+B_1^o-\check{k}^2B_0^o\tilde{z}.$$

Upon matching both solutions, we obtain the first order perturbation of the surface temperature

$$T_1^i(0)=C_1^i=C_1^o-\check{k}^2\int_0^\infty\tilde{z}u_0^i(\tilde{z})\,\mathrm{d}\tilde{z}, \tag{4.20}$$

where $C_1^o=-B_1^o+\cos(\alpha)(B_0^o\check{R}e_0+w_0^i(\infty)/\check{R}e_0)$. Using the representation

$$B_1^o=\check{k}^2B_{1,k}^o+\check{\lambda}_1B_{1,\omega}^o+\check{R}e_1B_{1,R}^o,$$

we find from the stress balance condition

$$\tilde{R}e_1=\tilde{R}e_0\left(\tfrac{1}{2}\check{\alpha}^2-\frac{\check{k}^2\tilde{B}_{1,k}^o+\check{\lambda}_1B_{1,\omega}^o+Pr^{1/4}\check{\alpha}B_{1,\alpha}^o}{2B_0^o+\check{R}e_0B_{1,R}^o}\right), \tag{4.21}$$

where $\tilde{B}_{1,k}^o=B_{1,k}^o+\int_0^\infty\tilde{z}u_0^i(\tilde{z})\,\mathrm{d}\tilde{z}$ and $B_{1,\alpha}^o=(B_0^o\check{R}e_0+w_0^i(\infty)/\check{R}e_0)$. The frequency correction follows from the requirement that the Reynolds number must be a real

quantity $\mathrm{Re}\,[\tilde{R}e_1] = 0$:

$$\breve{\omega}_1 = -\mathrm{Im}\left[\frac{\breve{k}^2\tilde{B}^o_{1,k} + Pr^{1/4}\breve{\alpha}B^o_{1,\alpha}}{2B^o_0 + Re_0B^o_{1,R}}\right] \Big/ \mathrm{Re}\left[\frac{B^o_{1,\omega}}{2B^o_0 + \breve{R}e_0B^o_{1,R}}\right] = \breve{k}^2\breve{\omega}_{1,k} + Pr^{1/4}\breve{\alpha}\breve{\omega}_{1,\alpha}.$$

Taking into account that $\breve{k}^2 = \breve{k}_x{}^2\breve{\alpha}^{-2}$ the critical angle defined by $\mathrm{d}\breve{R}e_1/\mathrm{d}\breve{\alpha} = 0$ is

$$\begin{aligned}\breve{\alpha}_c &= \breve{k}^{1/2}_{x,c}\left(-2\frac{\tilde{B}^o_{1,k} + \mathrm{i}\breve{\omega}_{1,k}}{2B^o_0 + \breve{R}e_0B^o_{1,R}}\right)^{1/4} + Pr^{1/4}\frac{1}{4}\frac{\tilde{B}^o_{1,\alpha} + \mathrm{i}\breve{\omega}_{1,\alpha}}{2B^o_0 + \breve{R}e_0B^o_{1,R}}\\ &= 1.316 + Pr^{1/4}1.72.\end{aligned}$$

Note that the last term $O(Pr^{1/4})$ in the above expression represents the next-order small correction which is still significant at $Pr \sim 10^{-3}$ where the asymptotic solution found begins to approach the corresponding numerical solution (see figure 9*a*). The critical wavelength defined by $\tilde{k}_c = \tilde{k}_{x,c}/\breve{\alpha}_c$ is plotted in figure 9(*b*) next to the corresponding numerical solution.

According to the solution obtained, flow disturbances extend from the free surface into the underlying liquid layer at the distance $\sim k_c^{-2} \sim Pr^{1/2}/Ha$. Thus, for the disturbances to decay before they encounter the bottom of the layer, the magnetic field must be strong enough such that $Ha \gg Pr^{-1/2}$. This is the condition required for the applicability of the Hartmann-layer model considered above.

4.2. *Oblique finite-depth mode for an insulating bottom*

Numerical solution of the complete problem indicates that for the Hartmann-layer mode to become the most dangerous one at small Prandtl numbers a strong magnetic field may be necessary. For instance, at $Pr \sim 10^{-2}$, $Ha \sim 10^2$ is required (see figures 7*a* and 9*a–c*). It means that in strong magnetic fields $Ha \gg 1$ but at sufficiently small Prandtl numbers the most unstable are instability modes extending over the whole depth of the layer. In this section, such an instability mode will be considered for the case of a thermally insulating bottom of the layer.

To simplify the analysis we again exploit a couple of useful facts suggested by the numerical solution of the full problem. First, the numerical solution indicates that the critical wavelength is considerably longer than the depth of the layer: $k \ll 1$. Second, the critical frequency is found to be much lower than the inverse viscous relaxation time over the thickness of the Hartmann layer but much higher than the same time over the depth of the layer: $1 \ll \omega \ll Ha^2$.

In order to use the results of the previous section, we shall employ the Hartmann-layer variables here also. The leading-order perturbation of the vertical velocity in the Hartmann layer at the free surface is governed by the same equation (4.1) as for the Hartmann-layer mode considered above. It is easy to find that the corresponding leading order solution in the Hartmann layer at the bottom is trivial: $w_0^-(z_-) \equiv 0$. Then the solution for the bulk of the layer, for which equation (2.10) turns to $\mathrm{d}^2w^o_0/\mathrm{d}z^2 = 0$, is $w^o_0(z) = w^i_0(\infty)(1/2 + z)$.

Now we proceed to the leading-order perturbation of the longitudinal velocity which is governed in the Hartmann layer at the free surface by equation (4.11). In the Hartmann layer at the bottom, where the coordinate is stretched as $z_- = Ha(1/2+z)$, equation (4.5) becomes

$$\frac{\mathrm{d}^2j_0^-}{\mathrm{d}z_-^2} = \mathrm{i}\frac{\mathrm{d}u_0^-}{\mathrm{d}z_-}.$$

The solution of the above equation satisfying the boundary condition $j_0^-(0) = 0$ is

$$j_0^-(z_-) = \mathrm{i}\int_0^{z_-} (u_0^-(\tau) - E_0^-)\,\mathrm{d}\tau.$$

Upon substituting the above result into equation (2.11), we obtain

$$\left[\frac{\mathrm{d}^2}{\mathrm{d}z_-^2} - 1\right] u_0^- = -E_0^-,$$

whose solution satisfying the no-slip condition at the bottom $u_0^-(0) = 0$ is

$$u_0^-(z_-) = E_0^-(1 - \mathrm{e}^{-z_-}).$$

In the bulk of the layer, equations (2.11) and (4.5) take the form

$$Ha\tilde{\lambda}u_0^o = \mathrm{i}\frac{\mathrm{d}j_0^o}{\mathrm{d}z}, \qquad \mathrm{i}Ha\frac{\mathrm{d}u_0^o}{\mathrm{d}z} = \frac{\mathrm{d}^2 j_0^o}{\mathrm{d}z^2}.$$

The solution of the above equations is $u_0^o(z) = B_0^o$ and $j_0^o(z) = -\mathrm{i}Ha\tilde{\lambda}(B_0^o + C_0^o)$. After matching the core velocity perturbation with that in the Hartmann layer at the bottom, we find $E_0^- = B_0^o$. Matching of the corresponding current perturbations $j_0^-(\infty) = -\mathrm{i}B_0^o = j_0^o(-\frac{1}{2})$ yields $C_0^o = B_0^o(\frac{1}{2} + Ha^{-1}\tilde{\lambda}^{-1})$. Finally, matching the core electric current perturbation with that of the Hartmann layer at the free surface $j_0^i(\infty) = -\mathrm{i}\int_0^\infty u_0^i(\tilde{z})\,\mathrm{d}\tilde{z} = j_0^o(\frac{1}{2})$ leads to

$$B_0^o = (Ha\tilde{\lambda} + 1)^{-1}\int_0^\infty u_0^i(\tilde{z})\,\mathrm{d}\tilde{z}. \tag{4.22}$$

Thus the perturbation of the longitudinal velocity in the bulk of the layer and in the Hartmann layer at the bottom is completely related to the perturbation in the Hartmann layer at the free surface.

Now it remains to find the temperature perturbation. For insulating boundaries, it is useful to search for the temperature perturbation in the form of the following power series of the Prandtl number: $T_0 = \sum_{m=0}^\infty Pr^{m-1}T_{0,m}$. Then the equation for the leading-order term of the above series takes the form $\mathrm{d}^2T_{0,0}/\mathrm{d}z^2 = 0$. Solution of this equation satisfying the adiabatic boundary conditions $T'_{0,0}(\pm\frac{1}{2}) = 0$ is a constant which can be determined by considering the problem for the next-order term:

$$\frac{\mathrm{d}^2T_{0,1}}{\mathrm{d}z^2} = -(\mathrm{i}\tilde{R}e^{-1}Ha^{-1} + \tilde{k}_y^2u_0(z)) + Ha^2(\tilde{\lambda} + Pr^{-1}\tilde{k}^2)T_{0,0}.$$

Integrating the above equation over the depth of the layer and taking into account adiabatic boundary conditions $T'_{0,1}(\pm\frac{1}{2}) = 0$, we obtain

$$T_{0,0} = \frac{Ha^{-2}\tilde{k}_y^2}{\tilde{\lambda} + Pr^{-1}\tilde{k}^2}\int_{-1/2}^{1/2} u_0(z)\,\mathrm{d}z.$$

Upon substituting the above result into the stress balance condition (2.13) and neglecting the contributions of both Hartmann layers in the above integral, we arrive at the following dispersion relation:

$$(\tilde{\lambda} + Pr^{-1}\tilde{k}^2)(Ha\tilde{\lambda} + 1) + (\tilde{k}_y\tilde{R}e)^2\int_0^\infty u_0^i(\tilde{z})\,\mathrm{d}\tilde{z} = 0, \tag{4.23}$$

which can be solved completely analytically by employing the last important numerical

implication: $\tilde{k}_x\tilde{R}e \ll 1$. Then straightforward but lengthy calculations give

$$\int_0^\infty u_0^i(\tilde{z})\,\mathrm{d}\tilde{z} = -\tfrac{1}{2} + \tfrac{19}{36}\mathrm{i}\tilde{k}_x\tilde{R}e - \tfrac{373}{864}(\mathrm{i}\tilde{k}_x\tilde{R}e)^2 + \tfrac{42127}{129600}(\mathrm{i}\tilde{k}_x\tilde{R}e)^3 + O((\mathrm{i}\tilde{k}_x\tilde{R}e)^4). \tag{4.24}$$

Note that we need all the four terms in the above series to find the leading-order solution of the stability problem under consideration. Before we proceed to the solution, it is worth noting that the Prandtl number can be eliminated from the problem by rescaling the wavenumber and the Reynolds number as follows:

$$\tilde{k} = Pr^{1/2}\check{k}, \qquad \tilde{R}e = Pr^{-1/2}\check{R}e.$$

The leading-order critical Reynolds number can be found by taking the first two terms of series (4.24). From the leading-order real and imaginary parts of the stress balance condition (4.23), we obtain, respectively, the following equations:

$$Ha\tilde{\omega}_0^2 = \tfrac{1}{2}(\check{k}_y\check{R}e_0)^2, \qquad Ha\tilde{\omega}_0\check{k}^2 = \tfrac{19}{36}\check{k}_x\check{k}_y^2\check{R}e_0^3,$$

which yield

$$\check{R}e_0 = 6(2^{1/2}/19)^{1/2}Ha^{1/4}\sin^{-1/2}(2\alpha), \tag{4.25}$$

$$\check{\omega}_0 = (2Ha)^{-1/2}\check{k}_y\check{R}e_0. \tag{4.26}$$

According to (4.25), the minimum of the Reynolds number

$$\check{R}e_{0,c} = 6(2^{1/2}/19)^{1/2}Ha^{1/4}$$

is attained at the critical angle $\alpha_c = \pi/4$. This is in good agreement with the numerically found critical angle plotted in figure 8(*b*) where the curve for $Pr = 10^{-2}$ and an insulating bottom closely approaches the critical angle 45° at $Ha \approx 200$ before the instability switches to the Hartmann-layer mode. Also the critical Reynolds number is seen in figure 8(*a*) (asymptotic 2) to approach the corresponding exact solution quite well.

The leading-order solution obtained leaves undetermined the critical wavenumber and so the critical frequency which according to equation (4.26) depends on it. To determine the critical wavenumber we have to take into account the next-order small correction to both real and imaginary parts given in the stress balance condition (4.23) by the third and fourth term of expansion (4.24). After some algebra, the next order correction to the Reynolds number is found as

$$\check{R}e_1 = (2\check{R}e_0)^{-1}\left(\tfrac{75587}{410400}Re_0^4\cos^2(\alpha)\check{k}^2 + Ha^{-1}Re_0^2\check{k}^{-2} + \sin^{-2}(\alpha)\right).$$

The critical wavenumber defined by the condition $\partial\check{R}e_1/\partial\check{k}|_{\alpha=\pi/4} = 0$ is found to be $\check{k}_c = 1.419Ha^{-3/8}$. The corresponding critical frequency is $\tilde{\omega}_{0,c} = 1.613Ha^{-5/8}$. These asymptotic solutions are seen in figures 9(*b*) and 9(*c*) close to the corresponding numerical results.

4.3. *Oblique finite-depth mode for a conducting bottom*

In this case, just as in the previous one, numerical results suggest a critical wavelength much longer than the characteristic thickness of the Hartmann layer but, conversely to the previous case, much shorter than the depth of the whole layer: $1 \ll k \ll Ha$. The frequency is implied to be lower than the inverse viscous relaxation time over the Hartmann layer, but higher than the corresponding time over the wavelength: $k^2 \ll \omega \ll Ha^2$. Upon such assumptions, the solution of the problem proceeds

identically to the previous case up to the finding of the temperature perturbation. In this case, the leading-order temperature perturbation is

$$T_0(z) = Ha^{-2}B_0^o \sin^2(\alpha)(1 - \cosh^{-1}(k)).$$

Neglecting the last term above which is exponentially small for $k \gg 1$, we arrive at the same leading-order stress balance condition as in the case of the Hartmann-layer mode given by equation (4.12). The problem under consideration is almost identical to that of the Hartmann-layer mode solved above, except for the relation between the longitudinal velocity perturbation in the bulk of the layer and that in the Hartmann layer at the free surface. In the case under consideration, this relation is defined by equation (4.22) instead of equation (4.10) used for the Hartmann-layer mode. Similarly as for the Hartmann-layer mode, the Prandtl number can be eliminated by rescaling the Reynolds number and the streamwise wavenumber according to transformations (4.13) and (4.14). In addition, we can also eliminate the Hartmann number entering relation (4.22) by rescaling the frequency as $\tilde{\omega} = Ha^{-1}\check{\omega}$. Because in the case under consideration $\tilde{k}_x Re \sim 1$, the problem is solved numerically similarly to the Hartmann-layer instability. The calculated leading-order marginal Marangoni number and the corresponding frequency are plotted versus the rescaled streamwise wavenumber in figure 11. The critical Marangoni number $Ma_c = 6.26Pr^{1/2}Ha^2$ is found to occur at the critical streamwise wavenumber $k_{x,c} = 0.54Pr^{1/2}Ha$ which is very close to the corresponding value for the Hartmann-layer instability. The critical frequency resulting from the leading order solution $\omega_c = 3.15Ha$ turns out to be about two times smaller than the corresponding numerical result. The discrepancy is due to the neglected higher-order small term $-Re/Ha^2$ in the basic flow (2.7) accounting for the return flow in the core of the layer. On one hand, this term represents a next-order small correction to the basic flow in the Hartmann layer. On the other hand, it is the dominating one in the core region where the leading term becomes exponentially small. However, the principal point is that this term being a constant additive to the basic flow can be eliminated by a proper change of the frame of reference. But this change has no effect on the stability of the flow. It only changes the relative phase speed of the disturbance and so the frequency by $Ha^{-2}Re_c k_{x,c} = 3.41Ha$. After taking into account this correction the resulting critical frequency agrees very well with the corresponding numerical one (see figure 9*c*).

Similarly to the Hartmann-layer mode, the leading-order solution yields only the streamwise component of the critical wavenumber while the next-order solution is necessary to determine the magnitude or the direction of the critical wave vector. Like the previous case, the next-order perturbation is due to the finite wavelength. But in this case, the dominating contribution comes from the perturbation of the longitudinal velocity in the core region

$$\check{\lambda}_0 u_1^o - \mathrm{i}\frac{\mathrm{d}j_1^o}{\mathrm{d}z_-} = -Ha^{-1}k^2 u_0^o - \check{\lambda}_1 u_0^o, \tag{4.27}$$

$$\mathrm{i}\frac{\mathrm{d}u_1^o}{\mathrm{d}z_-} = -Ha^{-1}k^2 j_0^o(z). \tag{4.28}$$

Thus the next-order perturbation is $\sim Ha^{-1}k^2$. Note that the corresponding effect in the Hartmann-layer leads to the correction $\sim \tilde{k}^2 \sim Ha^{-2}k^2$ which is a higher order small quantity compared to the former. Upon matching the solution of the above equations to the corresponding Hartmann-layer solutions at the bottom and the free

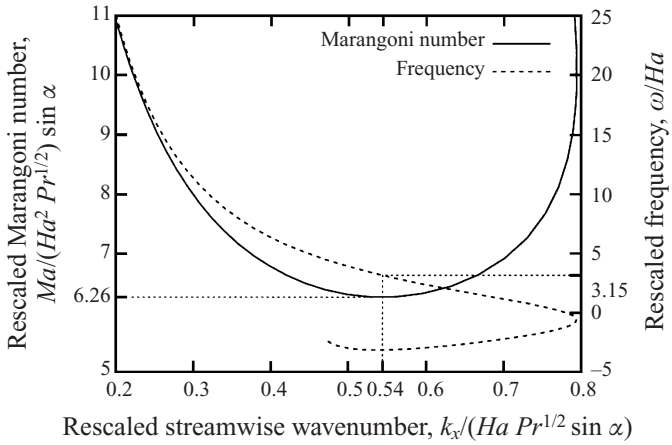

FIGURE 11. Leading-order rescaled marginal Marangoni number and rescaled frequency of the oblique wave mode versus rescaled streamwise wavenumber for the finite-depth mode at a conducting bottom and $Pr \ll Ha^{-2}$.

surface, we obtain

$$u_1^o(\tfrac{1}{2}) = \frac{1}{1+\breve{\lambda}_0}\left[\int_0^\infty u_1^i(\tau)\,\mathrm{d}\tau + B_0^o(Ha^{-1}k^2\breve{\lambda}_0(1+\breve{\lambda}_0/3) - \breve{\lambda}_1)\right],$$

where u_1^i is the corresponding perturbation of the longitudinal velocity in the Hartmann layer which, as usual, can be found numerically by solving equation (4.7) in which the core velocity perturbation at the free surface is defined by the above relation. Eventually, the next-order temperature perturbation of the free surface can be found as

$$T_1(\tfrac{1}{2}) = Ha^{-2}u_1^o(\tfrac{1}{2}) = Ha^{-2}(Ha^{-1}k^2B_{1,k}^o + \breve{\lambda}_1 B_{1,\omega}^o + \breve{R}e_1 B_{1,R}^o).$$

Substituting the above result into the stress balance condition (4.12) and taking into account a small exponential correction to the leading-order temperature perturbation we find the next-order correction to the marginal Reynolds number:

$$\tilde{R}e_1 = \tilde{R}e_0\left(\tfrac{1}{2}\breve{\alpha}^2 + \mathrm{e}^{-k} - \frac{Ha^{-1}k^2B_{1,k}^o + \breve{\lambda}_1 B_{1,\omega}^o}{2B_0^o + \tilde{R}e_1 B_{1,R}^o}\right).$$

The constraint $\mathrm{Im}\,[\tilde{R}e_1] = 0$ defines the frequency correction

$$\breve{\omega}_1 = -\mathrm{Im}\left[\frac{Ha^{-1}k^2\tilde{B}_{1,k}^o}{2B_0^o + Re_0B_{1,R}^o}\right] \Big/ \mathrm{Re}\left[\frac{B_{1,\omega}^o}{2B_0^o + \breve{R}e_0B_{1,R}^o}\right] = Ha^{-1}k^2\breve{\omega}_{1,k}.$$

Taking into account $\breve{\alpha} = k_x/k$, the condition $\mathrm{d}\tilde{R}e_1/\mathrm{d}k = 0$ leads to the following equation defining the critical wavenumber

$$k_x^2k^{-3} + \mathrm{e}^{-k} + 2Ha^{-1}k\frac{B_{1,k}^o + \mathrm{i}\breve{\omega}_{1,k}B_{1,\omega}^o}{2B_0^o + \breve{R}e_0B_{1,R}^o} = 0.$$

Neglecting the small exponential term, we find the leading-order solution for the

critical wavenumber

$$k_{c,0} = \left(-Hak_{x,c} \frac{2B_0^o + \check{R}e_0 B_{1,R}^o}{2(B_{1,k}^o + \mathrm{i}\check{\omega}_{1,k} B_{1,\omega}^o)} \right)^{1/4} = 0.68(Pr\,Ha^3)^{1/4}.$$

Since the critical wavenumber reduces with decrease of the Prandtl number, the exponential term in the above equation becomes significant at sufficiently small Prandtl numbers. The correction to the critical wavenumber due to the exponential term is found as

$$k_{c,1} = \frac{1}{4} \frac{k_{c,0}^4}{k_{x,c}^2} \mathrm{e}^{-k_{c,0}} = 0.186Ha\ \exp(-0.68(Pr\,Ha^3)^{1/4}).$$

With this correction the asymptotic solution for the critical wavenumber as well as the critical angle of the wave vector are in very good agreement with the corresponding numerical results (see figures 9*a* and 9*b*).

5. Summary and concluding remarks

The present study is concerned with the effect of a transverse magnetic field on the hydrothermal wave instability of thermocapillary-driven convection in a planar unbounded layer of an electrically conducting liquid heated from the side. First, we analyse the linear stability of longitudinal disturbances by making use of an analytically found dispersion relation. Second, we solve numerically the linear stability problem for oblique disturbances. Third, we use the information supplied by the numerical solutions and order-of-magnitude analysis to solve the corresponding linear stability problems asymptotically considering the Prandtl and Hartmann numbers as small and large parameters, respectively.

The magnetic field is found to have a stabilizing effect on the hydrothermal waves. In a sufficiently strong magnetic field, the critical temperature gradient is increased as the square of the field strength. So the critical frequency increases also while the critical wavelength decreases inversely with field strength. These relations can be directly deduced from the effect of the magnetic field on the basic flow which, in a strong magnetic field, forms a jet at the free surface with a characteristic thickness $\sim Ha^{-1}$. Thus the Marangoni number and frequency being proportional to the square of the characteristic length, both scale as $\sim Ha^2$, while the wavenumber, being directly proportional to the characteristic length, scales as $\sim Ha$.

The field strength at which these asymptotics become effective depends on the Prandtl number: the smaller the Prandtl number, the higher the field strength needed. This is related to the finite depth of the layer which, in addition to the thickness of the Hartmann layer, becomes a significant length scale at sufficiently small Prandtl numbers. For instance, longitudinal disturbances extend from the free surface into the depth of the layer at a distance comparable to the wavelength $\sim Pr^{-1/2}Ha^{-1}$ which is determined by the thermal diffusion time across the wave becoming comparable to the viscous diffusion time over the Hartmann layer. For the thickness of the Hartmann layer to be the only relevant length scale, disturbances should decay over a distance shorter than the depth of the layer which is the case provided $Ha \gg Pr^{-1/2}$. Note that in this case the critical frequency is higher than the inverse thermal diffusion time over the depth of the layer $\sim Pr^{-1}$. Thus the instability is insensitive not only to the depth of the layer but also to the actual thermal boundary conditions at the bottom. This changes at $Ha \sim Pr^{-1/2}$ where disturbances begin to extend over the

whole depth. For such instability modes the finite depth of the layer and the particular thermal boundary conditions at the bottom of the layer play an important role. As a result, the corresponding dependences of the critical parameters on the field strength are more complicated than for the instability modes related only to the Hartmann layer at the free surface.

Like the case without a magnetic field, the most unstable disturbances are oblique rather than longitudinal. In strong magnetic fields, when the instability is related to the Hartmann layer, the propagation angle depends solely on the Prandtl number. In this case the most unstable oblique waves become almost longitudinal at small Prandtl numbers. The leading-order asymptotic solution for such disturbances yields only the critical Marangoni number $Ma_c = 7.68Pr^{1/2}Ha^2$ and the streamwise component of the critical wavenumber $k_{x,c} = 0.716Pr^{1/2}Ha$ while the critical angle of propagation $\alpha_c = \pi/2 - 1.316Pr^{1/4} - 1.72Pr^{1/2}$ is determined by the next-order small effects. Oblique disturbances extend from the free surface into the depth of the layer over a distance exceeding the characteristic depth of the Hartmann layer by a factor $\sim k_c^{-2}$. Thus oblique disturbances cover the whole depth of the layer similarly to the longitudinal ones when $Pr \sim Ha^{-2}$. For smaller Prandtl numbers the finite depth of the layer becomes significant. However, the finite depth has no major effect on the leading-order asymptotic solutions for the critical Marangoni number $Ma_c = 6.26Pr^{1/2}Ha^2$ and the critical streamwise wavenumber $k_{x,c} = 0.54Pr^{1/2}Ha$ which are close to the corresponding values for the Hartmann-layer instability mode. The first significant difference from the Hartmann-layer mode concerns the critical frequency which in the latter case is found directly from the leading-order solution. Upon taking into account a correction due to the higher-order small term in the basic flow the leading-order critical frequency is found to be $\omega_c = 6.56Ha$. Similarly to the Hartmann-layer mode the critical wavenumber is determined by the solution next to the leading-order one which yields $k_c = 0.68(PrHa^3)^{1/4}$. However, the critical wavelength is still much shorter than the depth of the layer. Thus only the flow disturbances extend over the whole depth of the layer while the temperature disturbances, decaying over a characteristic distance comparable to the wavelength, remain confined at the free surface. As a result, this instability mode is rather insensitive to the actual thermal boundary conditions at the bottom of the layer. For instance, a perfectly conducting bottom gives rise to a higher-order small exponential correction to the critical wavenumber $k_{1,c} = 0.186Ha \exp(-0.68(PrHa)^{1/4})$. This correction becomes comparable to the leading-order result at small Prandtl numbers $Pr \sim Ha^{-3}\ln(Ha)$. Thus the above asymptotic solution for the finite depth mode at a conducting bottom turns out to be in good agreement with corresponding numerical results down to $Pr = 10^{-3}$ even at such moderate Hartmann numbers as $Ha = 10$.

In the case of a thermally insulating bottom at sufficiently small Prandtl numbers the most unstable mode is an oblique finite-depth mode which according to the leading order asymptotic solution propagates at an angle of 45° with respect to the basic flow. The corresponding critical Marangoni number is $Ma_c = 1.64Pr^{1/2}Ha^{9/4}$. The critical wavenumber $k_c = 1.42Pr^{1/2}Ha^{5/8}$ and the frequency $\omega_c = 1.61Ha^{11/8}$ are obtained by considering higher-order asymptotically small terms. This is a long-wave instability mode which disappears when $Pr \gtrsim Ha^{-5/4}$: the critical wavelength becomes comparable with the depth of the layer, and the instability switches to the Hartmann-layer mode.

Without a magnetic field, the obliqueness of the most unstable mode at small Prandtl numbers is related to the hydrodynamic stability of plane Couette flow (Priede & Gerbeth 1997*a*). It is well-known that plane Couette flow becomes linearly

unstable in a transverse magnetic field (Kakutani 1964) and that the Hartmann layer forming in a strong magnetic field is linearly unstable as well (Lock 1955). Since the critical Reynolds number for the oblique Hartmann-layer mode increases as $\sim Pr^{-1/2}$ one might expect a transverse hydrodynamic instability of the Hartmann layer to become the most unstable at sufficiently small Prandtl numbers. It turns out that the linear stability of the Hartmann layer strongly depends on the boundary conditions. For no-slip boundary conditions we found that the Hartmann layer becomes linearly unstable at a large but finite critical Reynolds number $\tilde{R}e_c = 48311$ in agreement with Lock (1955). In the case of a free-slip condition which holds for the flow disturbances at the free surface in the limit of $Pr = 0$ we found that the Hartmann layer is linearly stable, like Couette flow without a magnetic field. So the oblique mode remains the most unstable one at small Prandtl numbers in a strong magnetic field. However, we cannot exclude hydrodynamic instability due to the surface waves. In the same way as for the hydrodynamic mode of the Hartmann layer, it follows that the surface-wave instability, if any, would be the most dangerous mode at sufficiently small Prandtl numbers as found in the non-magnetic case by Smith & Davis (1983*b*). No further conclusions can be drawn about this instability mode in a magnetic field without its detailed analysis which, however, goes outside the scope of this paper.

In this study we have neglected the effect of buoyancy that under normal gravity requires the liquid layer to be thin enough. Without a magnetic field the ratio of the characteristic velocities of buoyancy- and thermocapillary-driven flows is given by the dynamic Bond number $Bo = g\alpha\rho d^2/\gamma$, where g and α are the gravitational acceleration and the volumetric expansion coefficient. For small-Prandtl-number liquids like common metal and semiconductor melts the effect of buoyancy on the hydrothermal wave instability is known to remain small up to $Bo \sim 1$ (Priede & Gerbeth 1997*c*) which restricts the maximal thickness of the layer to several millimetres. A magnetic field retarding buoyancy- and thermocapillary-driven flows as $\sim Ha^{-2}$ and $\sim Ha^{-1}$, respectively, reduces the relative effect of buoyancy as $\sim Bo/Ha$ (Ben Hadid, Henry & Kaddeche 1997). Thus for $Ha = 30$ buoyancy remains negligible up to layer depth of about 1 cm. For instance on a layer of liquid gallium ($Pr = 0.03$) of such a depth $Ha = 30$ is achieved at the induction of the magnetic field $B \approx 0.075\,\mathrm{T}$. In this case, according to our theory the most dangerous instability mode is the oblique finite-depth one. For a thermally insulating bottom wall the instability is expected to set in at a critical Marangoni number $Ma_c = 937.4$ that corresponds to a critical temperature gradient $\beta = 28.8\,\mathrm{K\,cm^{-1}}$. For a thermally well conducting bottom we have, respectively, $Ma_c = 1098.8$ and $\beta = 33.7\,\mathrm{K\,cm^{-1}}$. For the instability to be insensitive to the actual thermal boundary conditions at the bottom of the layer, $Ha > 71$ corresponding to $B > 0.18\,\mathrm{T}$ would be required. In this case the flow would become unstable at $Ma_c > 6300$ corresponding to $\beta > 193\,\mathrm{K\,cm^{-1}}$. According to these results the hydrothermal wave instability in a magnetic field could be observed in a terrestrial laboratory experiment.

The present study was concerned only with the conventional linear stability analysis predicting the threshold of the convective instability beyond which certain disturbances can be amplified. One must be aware that this instability may be not self-sustained and thus not observed in experiments without a permanent external excitation. For the thermocapillary-driven flow of low-Prandtl-number liquids without a magnetic field, the thresholds of absolute or global instabilities, which ensure development of self-sustained hydrothermal waves, are just slightly higher than the threshold of convective instability (Priede & Gerbeth 1997*c*). Whether this holds also with a magnetic field is not yet clear.

This work was supported by the German Space Agency (DARA).

Appendix. Asymptotic solutions for the longitudinal finite-depth modes

A.1. *Insulating bottom*

In this case, an asymptotic solution is sought directly by considering $1 \ll Ha \ll Pr^{-1/2}$ and assuming the most unstable disturbance to have a long wavelength $k \ll 1$. Since without the magnetic field the critical wave is long, for sufficiently small Pr we expect the wavelength to remain long up to a large enough Ha. This assumption is validated by the following solution. The hydrodynamic part of the problem is solved in general form for arbitrary frequency which will be specified further when considering particular instability modes.

Similarly to the case of the Hartmann-layer mode considered in § 3.1.2, equations (2.10)–(2.12) are solved by the method of matched asymptotic expansions. For this purpose, again we distinguish the Hartmann layer at the free surface where the coordinate is stretched as $z_+ = (\frac{1}{2} - z)Ha$. The vertical velocity at the free surface is found in the same way as in § 3.1.2, resulting in (3.8). For the Hartmann layer at the bottom another stretched coordinate $z_- = (\frac{1}{2} + z)Ha$ is introduced. It is easy to find that the solution for the leading-order vertical velocity at the bottom is trivial $w_0^-(z_-) \equiv 0$. Equation (2.10) written for the leading-order perturbation in the bulk of the layer takes the form $\mathrm{d}^2 w_0^o/\mathrm{d}z^2 = 0$ whose general solution is $w_0^o(z) = A_0^o + B_0^o z$. Matching of the core solution with both Hartmann layers yields $A_0^o = B_0^o/2 = \frac{1}{2}$. The corresponding composite solution is

$$w_0(z) = \tfrac{1}{2} + z - \exp\left(-(\tfrac{1}{2} - z)Ha\gamma_i\right). \tag{A 1}$$

Now we proceed to the leading-order perturbation of the longitudinal velocity for which upon twofold integration equation (2.11) takes the form

$$\left[\frac{\mathrm{d}^2}{\mathrm{d}z^2} - \lambda - Ha^2\right] u_0 = \bar{u}_0' w_0 - (Ha^2 + \lambda)(E_0 + F_0 z), \tag{A 2}$$

where E_0 and F_0 are constants of integration. The boundary conditions (2.16) now being

$$\left[\frac{\mathrm{d}^2}{\mathrm{d}z^2} - \lambda - Ha^2\right] u_0' = k_y \bar{u}' w_0' \quad \text{on } z = \pm\tfrac{1}{2},$$

require $F_0 = 0$, satisfying at once the boundary conditions at both the free surface and at the bottom. Analogously to the Hartmann-layer mode, this implies E_0 can be determined by some kind of solvability condition for the higher-order solution.

For the Hartmann layer at the bottom equation (A 2) takes the form

$$\left[\frac{\mathrm{d}^2}{\mathrm{d}z_-^2} - 1 - \tilde{\lambda}\right] u_0^- = -(1 + \tilde{\lambda})E_0,$$

whose solution bounded as $z_- \to \infty$ and satisfying the non-slip condition $u_0^-(0) = 0$ is

$$u_0^-(z_-) = E_0(1 - \mathrm{e}^{-\gamma_i z_-}).$$

The core solution is $u_0^o(z) = E_0$. For the Hartmann layer at the free surface equation (A 2) reads as

$$\left[\frac{\mathrm{d}^2}{\mathrm{d}z_+^2} - 1 - \tilde{\lambda}\right] u_0^+ = -\tilde{u}' w_0^+ - (1 + \tilde{\lambda})E_0$$

and has a bounded solution $u_0^+(z_+) = E_0 + F_0^+ \mathrm{e}^{-\gamma_i z_+} + u_{0,p}(z_+)$, where

$$u_{0,p}^+(z_+) = -\frac{1}{\gamma_i}\int^{z_+} \sinh\left(\gamma_i(z_+ - \tau)\right)\tilde{u}'(\tau)w_0^+(\tau)\,\tau.$$

The free-slip boundary condition $u_0^{+\prime}(0) = 0$ gives $F_0^+ = \gamma_i^{-1}u_{0,p}^{+\prime}(0)$. The composite solution is obtained as $u_0(z) = u_0^+(z_+) - E_0\mathrm{e}^{-\gamma_i z_-}$. To determine the unknown constant E_0, we have to consider the next order in k perturbation of the longitudinal velocity governed by

$$\frac{\mathrm{d}^2}{\mathrm{d}z^2}\left[\frac{\mathrm{d}^2}{\mathrm{d}z^2} - \lambda - Ha^2\right]u_1 = \frac{\mathrm{d}^2}{\mathrm{d}z^2}\left[\bar{u}'w_1\right] + k^2\left[\frac{\mathrm{d}^2u_0}{\mathrm{d}z^2} + Ha^2u_0 - (\lambda + Ha^2)E_0\right].$$

Integrating this equation over the depth of the layer and taking into account boundary conditions (2.16), now being

$$\left[\frac{\mathrm{d}^2}{\mathrm{d}z^2} - \lambda - Ha^2\right]u_1' = k_y\bar{u}'w_1' \quad \text{on } z = \pm\tfrac{1}{2},$$

we obtain the following constraint:

$$\int_{-1/2}^{1/2}(u_0(z) - (1+\tilde{\lambda})E_0)\,\mathrm{d}z = 0,$$

which must be satisfied for the above problem to be solvable for u_1. This yields

$$E_0 = -\frac{Re}{Ha^3}\frac{\gamma_i}{(\tilde{\lambda} + Ha^{-1}\gamma_i^{-1})(1+\tilde{\lambda})(1+\gamma_i)} = \frac{Re}{Ha^3}E_1, \tag{A 3}$$

which completes the leading-order solution for the longitudinal velocity.

A.1.1. *Low-frequency instability*

Now we proceed to the leading-order temperature perturbation governed by

$$\left[Pr^{-1}\mathbf{D}^2 - \lambda\right]T_0 = -u_0, \tag{A 4}$$

and satisfying $T_0'(\pm\frac{1}{2}) = 0$ at both boundaries assumed to be adiabatically insulated. Following the case without magnetic field (Priede & Gerbeth 1997*b*), we assume here the critical frequency to be low compared to the inverse characteristic thermal relaxation time over the depth of the layer: $\omega \ll Pr^{-1}$. Then the temperature perturbation may be sought as

$$T_0(z) = \sum_{n=0}^{\infty} Pr^n T_{0,n}(z).$$

For the leading-order term equation (A 4) is $\mathrm{d}^2T_{0,0}/\mathrm{d}z^2 = 0$, whose solution satisfying adiabatic boundary conditions is $T_{0,0} = \text{const}$. The relation of this solution with the velocity perturbation is given by the solvability condition for the next-order temperature perturbation for which equation (A 4) takes the form

$$\frac{\mathrm{d}^2T_{0,1}}{\mathrm{d}z^2} = -u_0(z) + (\lambda + Pr^{-1}k^2)T_{0,0}.$$

After integration of the above equation over the depth of the layer with adiabatic boundary conditions, we find

$$T_{0,0} = \frac{1}{\lambda + Pr^{-1}k^2}\int_{-1/2}^{1/2} u_0(z)\,\mathrm{d}z = E_0\frac{1+\tilde{\lambda}}{\lambda + Pr^{-1}k^2}.$$

Now it remains to substitute this solution into the stress balance condition (2.13). Considering $\tilde{\omega} \ll 1$, we obtain

$$\begin{aligned} Re^2 &= \frac{Ha^5}{k^2}(\lambda + Pr^{-1}k^2)/E_1 \\ &\approx -\frac{Ha}{k^2}(2Ha^2\lambda^2 + Pr^{-1}k^2(2Ha^3 + \tfrac{3}{2}\lambda^2) + Ha^{-2}\lambda(2Ha^3 + \tfrac{3}{2}\lambda^2 + 2Ha^2Pr^{-1}k^2)). \end{aligned}$$

Since the marginal Reynolds number must be a real quantity, the frequency of neutrally stable waves is determined by requiring the imaginary part of the right-hand side of the above expression to be zero which yields

$$\omega = \frac{2}{\sqrt{3}}Ha(Ha + Pr^{-1}k^2)^{1/2}. \tag{A 5}$$

Then the marginal Reynolds number is

$$Re = Ha^{5/2}\left(\tfrac{8}{3}(Hak^{-2} + Pr^{-1}) + 2(PrHa)^{-2}k^2\right)^{1/2}. \tag{A 6}$$

The critical wavenumber at which the marginal Reynolds number attains its minimum is defined by $\mathrm{d}Re/\mathrm{d}k|_{k=k_c} = 0$.

A.1.2. *Intermediate-frequency instability*

Here we consider the thermal relaxation time to be comparable to the period of oscillations, meaning that the temperature perturbations spread from the free surface only over the thermal oscillatory boundary rather than over the whole liquid layer. Our aim here is to find an asymptotic solution of equation (A 4) which is singularly perturbed now. In line with the method of matched asymptotic expansions, the liquid layer is divided into a core region and thermal boundary layers at the free surface and at the bottom. In the core region, where the heat diffusion over the depth of the layer is negligible, the temperature perturbation is found as $T_0^o = E_0 Pr/\gamma_t^2$, where $\gamma_t = (\lambda Pr + k^2)^{1/2}$. For the thermal boundary layer at the free surface, we introduce a stretched coordinate $\zeta = (\frac{1}{2} - z)\gamma_t$, in terms of which equation (A 4) is

$$\left[\frac{\mathrm{d}^2}{\mathrm{d}\zeta^2} - 1\right] T_0^+ = -E_0 Pr\gamma_t^{-2}.$$

A bounded solution of this equation is $T_0^i(\zeta) = E_0 Pr\gamma_t^{-2} + F_0^i \mathrm{e}^{-\zeta}$. Now it remains to consider the Hartmann layer at the free surface, for which the coordinate is stretched as $z_+ = (\frac{1}{2} - z)Ha$, and the solution is sought as $T_0(z) = T_0^o + T_0^+(z_+)$. Then equation (A 4) takes the form

$$\frac{\mathrm{d}^2 T_0^+}{\mathrm{d}z_+^2} = -PrHa^{-2}(u_0^+(z_+) - E_0)$$

and can be solved as

$$T_0^+(z_+) = F_0^+ + PrHa^{-2}\theta_0^+(z_+),$$

where the particular solution is $\theta_0^+(z_+) = -\int_\infty^{z_+}(z_+ - \tau)(u_0^+(\tau) - E_0)\,\mathrm{d}\tau$. After matching the Hartmann- and thermal-layer solutions $T_0^o + T_0^+(\infty) = T_0^i(0)$, we obtain $F_0^+ =$

$F_0^i = F_0$. The composite solution may be written as

$$T_0(z) = E_0 Pr\gamma_t^{-2} + F_0 e^{-\zeta} + PrHa^{-2}\theta_0^+(z_+).$$

The last unknown coefficient F_0 is determined from the boundary condition $T_0'(1/2) = 0$

$$F_0 = Pr\gamma_t^{-1}Ha^{-1}\theta_0^{+\prime}(0) = Pr\gamma_t^{-1}(\tilde{\lambda} + Ha^{-1}\gamma_i^{-1})E_0.$$

Now the leading-order perturbation of the surface temperature can be evaluated as

$$T_0(1/2) \approx -\frac{1}{2}\frac{PrRe}{Ha^3}\frac{\gamma_i^2}{\gamma_t^2}\left(\frac{1}{\tilde{\lambda}} - \frac{7}{4} - \frac{Ha^{-1}}{\tilde{\lambda}^2} + (\tilde{\lambda}Pr)^{1/2}Ha\right).$$

Substituting the above solution together with that for the vertical velocity (A 1) into the stress balance condition (2.13), we obtain the dispersion relation sought whose imaginary part written in leading-order terms is

$$\frac{7}{4} - \frac{Ha^3}{\omega^2} - \left(\frac{Pr\omega}{2}\right)^{1/2} - k^2\frac{Ha^2}{Pr\omega^2} = 0. \tag{A 7}$$

In the long-wave limit $k = 0$, this equation relating the frequency and wavenumber of neutrally stable waves gives two different modes with frequencies $\omega_1 \approx 2/\sqrt{7}Ha^{3/2}$ and $\omega_2 \approx 49/8Pr^{-1}$. Both these modes merge together and disappear when the Hartmann number becomes sufficiently large $Ha \sim Pr^{-2/3}$. Note that the frequency of the first mode is considerably lower than the inverse thermal relaxation time over the depth of the layer. Thus the assumption $\omega \gtrsim Pr^{-1}$ employed to obtain this solution does not hold for this mode. It means that by assuming the heat disturbances to spread over the thermal boundary layer, whose thickness turns out to be considerably larger than the actual depth of the liquid layer, we have underestimated the effect of these disturbances on the perturbation of the surface temperature. However, comparing ω_1 with the corresponding exact result given by equation (A 5) at $k = 0$, we see that the difference between the two is just a factor $(\frac{3}{7})^{1/2}$. Thus for such low frequencies as ω_1 the contribution of the heat disturbances in the Hartmann layer at the free surface has no effect on the asymptotics of the solution. As for the other mode, $\omega_2 \sim Pr^{-1}$ is the frequency at which the thermal boundary layer at the free surface is anticipated to appear. Thus for the second mode our approach gives at least a qualitatively correct result as well. Consequently, despite some quantitative inaccuracy for the first mode the given approach is expected to be qualitatively correct and therefore able to recover the asymptotics of the corresponding exact solution.

Further, it is advantageous to consider equation (A 7) to define the wavenumber as a function of the frequency:

$$k(\omega) = \frac{Pr^{1/2}}{Ha}\left(\tfrac{7}{4}\omega^2 - \left(\frac{Pr\omega^5}{2}\right)^{1/2} - Ha^3\right)^{1/2}. \tag{A 8}$$

According to the above equation, two instability modes exist only for sufficiently long waves. Both modes merge together and disappear at the frequency at which k attains a maximum. From the condition $\mathrm{d}k/\mathrm{d}\omega = 0$ defining this maximum, the frequency at the merging point is found to be $\omega_* = \frac{98}{25}Pr^{-1}$. The corresponding wavenumber is

$$k_* = Ha^{-1}Pr^{-1/2}\left(\left(\tfrac{7}{5}\right)^5 - Ha^3Pr^2\right)^{1/2}. \tag{A 9}$$

Both modes disappear completely when the merging point shifts to infinitely long

waves $k_* = 0$ which happens at $Ha_* = \left(\frac{7}{5}\right)^{5/3} Pr^{-2/3}$. This result confirms the corresponding estimate found above.

A.2. *Conducting bottom*

There are two important facts for the asymptotic analysis suggested by the order-of-magnitude estimates. For the sake of brevity, in the following solution we shall directly exploit only the estimate $k \sim 1$ while the presence of an oscillatory sub-layer inside the Hartmann layer suggested by $\omega \gg Ha^2$ will not be explicitly used in the course of solution until the dispersion relation is obtained.

As was done above, the leading-order perturbation of the vertical velocity is readily found to be

$$w_0(z) = \frac{\sinh(\gamma_o(\frac{1}{2}+z))}{\sinh(\gamma_o)} - w_0^+(z_+) - 1,$$

where $w_0^+(z_+) = 1 - \mathrm{e}^{-\gamma_i z_+}$ is the Hartmann-layer solution, $\gamma_o = k(\tilde{\lambda}/(1+\tilde{\lambda}))^{1/2}$, $\gamma_i = (1+\tilde{\lambda})^{1/2}$, and $z_+ = Ha(\frac{1}{2} - z)$.

To simplify matching of the longitudinal velocity it is advantageous to rewrite equation (2.11) as a set of two equations using the vertical component of the induced electric current perturbation $\hat{j}$:

$$\left[\mathbf{D}^2 - \lambda\right]\hat{u} - k\bar{u}'\hat{w} + \mathrm{i}Ha(\boldsymbol{e}_z \cdot \mathbf{D})\hat{j} = 0, \tag{A 10}$$

$$\mathrm{i}Ha(\boldsymbol{e}_z \cdot \mathbf{D})\hat{u} = \mathbf{D}^2\hat{j}. \tag{A 11}$$

For the Hartmann layer at the free surface, equation (A 11) takes the form

$$\mathrm{i}\frac{\mathrm{d}u_0^+}{\mathrm{d}z_+} = \frac{\mathrm{d}^2 j_0^+}{\mathrm{d}z_+^2},$$

whose solution satisfying the boundary condition $j_0^+(0) = 0$ may be written as

$$j_0^+(z_+) = \mathrm{i}\int_0^{z_+} (u_0^+(\tau) - E_0^+)\,\mathrm{d}\tau,$$

where E_0^+ is a constant of integration. Substituting this solution into equation (A 10), we obtain for the Hartmann layer at the free surface

$$\left[\frac{\mathrm{d}^2}{\mathrm{d}z_+^2} - 1 - \tilde{\lambda}\right] u_0^+ = -k\tilde{u}' w_0^+ - E_0^+.$$

The solution of the above equation may be written as

$$u_0^+(z_+) = G_0^+ \mathrm{e}^{-\gamma_i z_+} + E_0^+/(1+\tilde{\lambda}) + u_{0,p}^+(z_+),$$

where $u_{0,p}^+(z_+) = -(k/\gamma_i)\int^{z_+} \sinh(\gamma_i(z_+ - \tau))\tilde{u}'(\tau) w_0^+(\tau)\,\mathrm{d}\tau$ is the particular solution; $G_0^+ = u_{0,p}^{+\prime}(0)/\gamma_i$ because of the boundary condition $u_0^{+\prime}(0) = 0$.

Similarly, for the Hartmann layer at the bottom we obtain

$$j_0^-(z_-) = -\mathrm{i}\int_0^{z_-} (u_0^-(\tau) - E_0^-)\,\mathrm{d}\tau,$$

$$u_0^-(z_-) = G_0^- \mathrm{e}^{-\gamma_i z_-} + E_0^-/(1+\tilde{\lambda}).$$

For the core region where equations (A 10), (A 11) take the form

$$Ha\tilde{\lambda}u_0^o = -\mathrm{i}\frac{\mathrm{d}j_0^o}{\mathrm{d}z}, \qquad -\mathrm{i}Ha\frac{\mathrm{d}u_0^o}{\mathrm{d}z} = \mathbf{D}^2 j_0^o,$$

the general solution may be obtained as

$$u_0^o(z) = G_0^o \sinh(\gamma_o(\tfrac{1}{2}+z)) + H_0^o \sinh(\gamma_o(\tfrac{1}{2}-z)),$$

$$j_0^o(z) = \mathrm{i}Ha\tilde{\lambda}/\gamma_o(G_0^o \cosh(\gamma_o(\tfrac{1}{2}+z)) - H_0^o \cosh(\gamma_o(\tfrac{1}{2}-z)).$$

Matching of velocity perturbations between the core region and both Hartmann layers yields $G_0^o/E_0^+ = H_0^o/E_0^- = [(1+\tilde{\lambda})\sinh(\gamma_o)]^{-1}$. After matching the electric current perturbations, we find $E_0^- = 0$ and

$$E_0^+ = \frac{k\gamma_o \tanh(\gamma_o)}{Ha\tilde{\lambda}} \int_0^\infty \tilde{u}'(\tau) w_0^+(\tau)\,\mathrm{d}\tau = -\frac{Re}{Ha^3}\frac{k^2 \tanh(\tilde{\gamma}_o)}{\tilde{\lambda}^{1/2}(1+\gamma_i)}.$$

Now we can proceed to the temperature perturbation for which equation (2.12) in the Hartmann layer at the free surface takes the form

$$\frac{\mathrm{d}^2 T_0^+}{\mathrm{d}z_+^2} = -PrHa^{-2}k^{-1}u_0^+(z_+).$$

The solution of the above equation satisfying the boundary condition $T_0^{+\prime}(0) = 0$ is

$$T_0^+(z_+) = I_0^+ - PrHa^{-2}k^{-1}\int_0^{z_+}(z_+ - \tau)u_0^+(\tau)\,\mathrm{d}\tau.$$

Equation (2.12) for the core region

$$\left[\frac{\mathrm{d}^2}{\mathrm{d}z^2} - k^2 - Pr\lambda\right] T_0^o = -Pr u_0^o(z) = -Pr G_0^o \sinh(\gamma_o(\tfrac{1}{2}+z))$$

has a solution

$$T_0^o(z) = I_0^o \sinh(\gamma_t(\tfrac{1}{2}+z)) - Pr G_0^+ \frac{\sinh(\gamma_o(\tfrac{1}{2}+z))}{\gamma_o^2 - \gamma_t^2},$$

satisfying the boundary condition $T_0^o(-\tfrac{1}{2}) = 0$, where $\gamma_t = (k^2 + Pr\lambda)^{1/2}$. Note that the Hartmann layer at the bottom is neglected here because it gives a higher order small correction to the temperature perturbation. After matching the Hartmann layer and the core temperature perturbations, we find

$$T_0(\tfrac{1}{2}) = \frac{PrReHa^{-3}k}{\tilde{\lambda}^{1/2}(1+\tilde{\lambda})(1+\gamma_i)}\left[\frac{\tanh(\gamma_o)}{\gamma_o^2-\gamma_t^2} - \frac{\tanh(\gamma_t)}{\gamma_t}\left(\frac{\tilde{\lambda}}{\gamma_o} - \frac{\gamma_o}{\gamma_o^2-\gamma_t^2}\right)\right].$$

Substituting the above result into the stress balance condition (2.13) and taking into account that according to the order-of-magnitude estimates $1 \ll \tilde{\lambda} \ll Pr^{-1}Ha^{-2}$, we obtain the following leading-order solutions for the marginal Reynolds number and the corresponding frequency:

$$Re = \tilde{\omega}(k)\left(\frac{Ha^5}{Prk\tanh(k)}\right)^{1/2}, \qquad \tilde{\omega}(k) = \left(\frac{k^3 + 3k^2\sinh(2k)}{PrHa^2\sqrt{2}(\sinh(2k) - 2k)}\right)^{2/3}.$$

REFERENCES

Ben Hadid, H., Henry, D. & Kaddeche, S. 1997 Numerical study of convection in the horizontal Bridgman configuration under the action of a constant magnetic field. Part 1. Two-dimensional flow. *J. Fluid Mech.* **33**, 23–56.

Canuto, C., Hussaini, M. Y., Quarteroni, A. & Zang, T. A. Jr 1988 *Spectral Methods in Fluid Dynamics*. Springer.

Davis, S. H. 1987 Thermocapillary instabilities. *Ann. Rev. Fluid Mech.* **19**, 403–435.

Gardner, D. R., Trogdon, S. A. & Douglass, R. W. 1989 A modified tau spectral method that eliminates spurious eigenvalues. *J. Comput. Phys.* **80**, 137–167.

Kakutani, T. 1964 The hydrodynamic stability of the modified plane Couette flow in the presence of a transverse magnetic field. *J. Phys. Soc. Japan* **19**, 1041–1057.

Lock, R. C. 1955 The stability of the flow of an electrically conducting fluid between parallel planes under a transverse magnetic field. *Proc. R. Soc. Lond.* A **233**, 105–125.

Maekawa, T. & Tanasawa, I. 1989 Effect of magnetic field and buoyancy on onset of Marangoni convection. *Intl J. Heat Mass Transfer* **32**, 1377–1380.

Moreau, R. 1990 *Magnetohydrodynamics*. Kluwer.

Nield, D. A. 1966 Surface tension and buoyancy effects in the cellular convection of electrically conducting liquid in a magnetic field. *Z. Angew. Math. Physik* **17**, 131–139.

Nitschke, K., Thess, A. & Gerbeth, G. 1991 Linear stability of Marangoni–Hartmann convection, In *Microgravity Fluid Mechanics* (ed. H. J. Rath); *Proc. IUTAM Symposium, Bremen 1991*, pp. 285–296. Springer.

Pearson, J. R. A. 1958 On convection cells induced by surface tension. *J. Fluid Mech.* **4**, 489–500.

Priede, J. & Gerbeth, G. 1997*a* Hydrothermal wave instability of thermocapillary-driven convection in a coplanar magnetic field. *J. Fluid Mech.* **347**, 141–169.

Priede, J. & Gerbeth, G. 1997*b* Influence of thermal boundary conditions on the stability of thermocapillary-driven convection at low Prandtl numbers. *Phys. Fluids* **9**, 1621–1634.

Priede, J. & Gerbeth, G. 1997*c* Convective, absolute, and global instabilities of thermocapillary–buoyancy convection in extended layers. *Phys. Rev.* E **56**, 4187–4199.

Priede, J., Thess, A. & Gerbeth, G. 1994 Thermocapillary instabilities in liquid metals: Hartmann-number versus Prandtl-number. In *Second Intl Conf. on Energy Transfer in Magnetohydrodynamic Flows, Aussois, France*, pp. 571–580.

Sarma, G. S. R. 1979 Marangoni convection in a fluid layer under the action of a transverse magnetic field. *Space Res.* **19**, 575–578.

Schwabe, D. 1988 Surface-tension-driven flows in crystal growth melts. In *Crystals*, vol. 7. Springer.

Series, R. W. & Hurle, D. T. J. 1991 The use of magnetic fields in semiconductor crystal growth. *J. Cryst. Growth* **113**, 305–328.

Smith, M. K. 1986 Instability mechanism in dynamic thermocapillary liquid layers. *Phys. Fluids* **29**, 3182–3186.

Smith, M. K. & Davis, S. H. 1983*a* Instabilities of dynamic thermocapillary liquid layers. Part 1. Convective instabilities. *J. Fluid Mech.* **132**, 119–144.

Smith, M. K. & Davis, S. H. 1983*b* Instabilities of dynamic thermocapillary liquid layers. Part 2. Surface-wave instabilities. *J. Fluid Mech.* **132**, 145–.

Takashima, M. 1981 Surface tension driven instabilities in a horizontal liquid layer with a deformable free surface. II. Overstability. *J. Phys. Soc. Japan* **50**, 2751–2756.

Wilson, S. K. 1993*a* The effect of a uniform magnetic field on the onset of steady Bénard–Marangoni convection in a layer of conducting fluid. *J. Engng Maths* **27**, 161–188.

Wilson, S. K. 1993*b* The effect of a uniform magnetic field on the onset of Marangoni convection in a layer of conducting fluid, *Q. J. Mech. Appl. Maths* **46**, 211–248.